Journal of Hydrology xxx (2011) xxx–xxx

Contents lists available at ScienceDirect

Journal of Hydrology

journal homepage: www.elsevier.com/locate/jhydrol

A survey of groundwater levels and hydrogeochemistry in irrigated fields in the Karamay Agricultural Development Area, northwest China: Implications for soil and groundwater salinity resulting from surface water transfer for irrigation

Dongmei Han [a], Xianfang Song [a,*], Matthew J. Currell [b], Guoliang Cao [c], Yinghua Zhang [a], Yuehu Kang [a]

[a] Key Laboratory of Water Cycle & Related Land Surface Processes, Institute of Geographic Sciences and Natural Resources Research, Chinese Academy of Sciences, Beijing 100101, China
[b] School of Civil, Environmental and Chemical Engineering, RMIT University, Melbourne 3001, Australia
[c] Department of Geological Sciences, University of Alabama, Tuscaloosa, AL 35487, USA

ARTICLE INFO

Article history:
Received 24 November 2010
Received in revised form 8 February 2011
Accepted 12 March 2011
Available online xxxx
This manuscript was handled by L. Charlet, Editor-in-Chief, with the assistance of P.J. Depetris, Associate Editor

Keywords:
Arid region
Groundwater storage
Irrigation
Hydrochemistry
Stable isotope

SUMMARY

Analysis of the water budget, along with hydrochemistry and stable isotopes in shallow groundwater were carried out in the Karamay Agricultural Development Area (KADA) in order to assess the impact of transfer of irrigation water from the IrtySh River, in particular in relation to the mechanisms of salinization and the nature of the water table regime. In terms of aquifer dynamics, the addition of the irrigation water without any groundwater abstraction has caused a sharp rise in the water table is and the development of serious soil salinity, together with an almost complete attenuation of inter-seasonal water table oscillations. The mean rise in the groundwater table from September 1997 to October 2009 was 6.9 m, representing an accumulated total water storage change of close to 150 million cubic meters. The analysis of aquifer water budget shows that infiltration of irrigation water occupied over 90% of the total recharge of the groundwater in the KADA. Sources of groundwater recharge and mechanisms of salinization in the KADA were also investigated using geochemical and isotopic techniques. The groundwater is characterized by $Cl(SO_4)$–Na type, generally becoming more Na and Cl dominated with increasing salinity. The total dissolved solids (TDS) content of the groundwater ranges from 0.5 g/L to over 65 g/L, with greater TDS values in areas of low topographic relief and shallow water tables. Where the sediments are more permeable (e.g. due to the presence of palaeochannels), TDS values are generally lower and the seasonal water table fluctuations greater. The ratios of K/Cl, Ca/Cl, Na/Cl, and Mg/Cl decrease with increasing Cl^- concentrations especially in the shallow groundwater from 10 to 15 m depth, indicating hydrogeochemical evolution via minor water-rock interaction (feldspar weathering) and significant evaporation. The stable isotopic compositions show a characteristic evaporation effect in the shallow groundwater and confirm that direct infiltration of precipitation is generally not a volumetrically important source of recharge to the shallow aquifer. Preferential recharge of river water after irrigation events and/or precipitation from rare heavy rain events is likely responsible for the depleted δ^2H and $\delta^{18}O$ values in some of the groundwater samples. The negative relationship between deuterium excess and $\delta^{18}O$ values indicates that even in groundwater with relatively depleted δ^2H and $\delta^{18}O$ values, evaporation has occurred to a significant degree. Careful management of water quantity and quality and implementation of salinity management strategies are considered necessary in order to reduce the risk of further salt accumulation and damage to farming and local ecosystems.

1. Introduction

Water scarcity is most acute in arid and semiarid regions, which cover almost one third of the Earth's land surface (Froehlich and Yurtsever, 1995). Due to water shortage, the extreme climate and vulnerable eco-environments in arid regions, particularly in the northwest of China, certain eco-environmental problems, caused by the exploitation and utilization of water resources (e.g., saline soils, rising groundwater levels, water quality problems) have become ubiquitous and continue to be an important topic of worldwide study.

The Kalamay agricultural development area (KADA) is located on a 194.3 km^2 alluvial plain situated in the northwest margin of the Junggar Basin, Xinjiang province and is one of the most arid regions in the northwest of China. It is characterized by low precipitation, high evapotranspiration and strong winds. The area is

* Corresponding author. Present address: Jia11#, Datun Road, Chaoyang District,100101 Beijing, PR China. Tel./fax: +86 10 64889849.
E-mail address: songxf@igsnrr.ac.cn (X. Song).

0022-1694/$ - see front matter © 2011 Elsevier B.V. All rights reserved.
doi:10.1016/j.jhydrol.2011.03.052

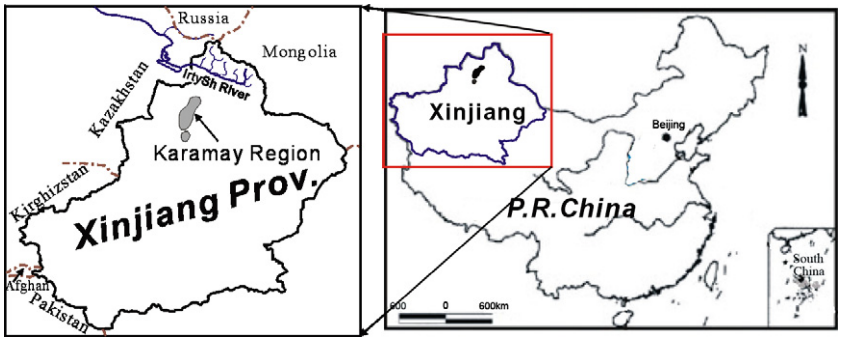

Fig. 1. Location of the IrtySh River and Karamay Region in Xinjiang Province of China.

characterized by groundwater with high total dissolved solids (TDS), low soil fertility, and serious soil salinization. There is no flow of surface water through the KADA, and high intensity rainfall events are very infrequent, hence there is very little available water for domestic, agricultural or industrial uses.

Fresh water scarcity is a limiting factor for agricultural and economic development in this region of China. There is current bureaucratic focus on settlement and development of China's mainly arid western provinces, which are less economically developed relative to eastern China. Since 2000, with the development of land in KADA for agricultural exploitation, irrigation has depended entirely on water transferred from IrtySh River, which is approximately 300 km away to the north of Kalamay (Fig. 1) and receives snowmelt from the mountains of northernmost Xinjiang. With the development of dams and water-transfer infrastructure since 2000, there have been projected to be 260 million m^3/a of water transferred to the KADA, with 140 million m^3/a earmarked for agriculture (mostly irrigated cotton growing), and 120 million m^3/a for domestic and industrial use. Extensive irrigation without adequate drainage has caused rising groundwater levels and upset the pre-existing water-salt balance in the soil zone and shallow aquifer. Previous research indicates that groundwater levels in the KADA have gradually risen since the beginning of irrigated agriculture (Yao et al., 2008). As water levels rise, dissolved salts move by capillary action to the shallow subsurface, and when the water evaporates, salts are left behind, causing degradation of the soil. This is similar to the mechanism which caused dryland salinity over large areas of the Murray Basin in Australia, which led to extensive damage to productive farmland in irrigated areas over the latter half of the 20th century (Arad and Evans, 1987; Allison et al., 1990; Simpson and Herczeg, 1991; Cartwright et al., 2007). If the situation in the Kalamay region continues, then there is a high likelihood that the fragile water–soil environment will deteriorate, and salinization will damage large areas of potential farmland in northwest China. It is thus necessary to discuss how to control the rising groundwater levels in this area.

This study is based on hydrogeological field surveys, including direct information from measurement of groundwater levels and indirect information from hydrochemical and isotope data. This enables the characterization of aquifer hydraulic characteristics, including groundwater recharge and discharge conditions. The purpose of the present study is to examine the relationships between changes in groundwater levels, shallow groundwater storage, and hydrogeochemistry in the KADA, where extensive irrigation is supported by transfer of surface water from outside the region, and to use these data to discriminate the local and regional causes of groundwater and soil salinisation. The research is expected to provide information that can be used to improve water resource management in anthropogenic oases that are being developed in arid and semi-arid regions, a particularly common occurrence in northwestern China in recent years. It is hoped that this can lead to better water and soil conservation and particularly, salinity control in KADA and other analogous regions.

2. Study area

KADA covers 194.3 km^2 and is situated on the Lacustrine plain in the northwestern Junggar Basin of Xinjiang, between 84°50′and 85°20′E and 45°22′–45°40′, southeast of the Zhayir Mountains. The study area is located 20 km from Kalamay city. Due to the high level of water utilization in the upper-reaches of the Manas River, which lies on the south of KADA, there has been no surface water flow through the area since the 1970s. The dried Manasi Lake is the major drainage area (Fig. 2). The elevation of the study area ranges from 268 m to 288 m above mean sea level, with a mean land surface slope of 0.26‰ from southwest to northeast.

The study area has a continental arid desert climate with average annual rainfall of approximately 111 mm, and approximately 70% of annual rainfall is received during the three-month period between July and September. Average annual water surface evaporation, measured with a 20 cm diameter evaporation pan, is approximately 3545 mm (Yao et al., 2008). The mean annual air temperature is 8.5 °C, with a maximum of 42.9 °C in July and minimum of −35.9 °C in January, while the maximum wind velocity is 49 m/s. The sunshine duration is 2734.6 h, and the percentage of sunshine is up to 61% with global solar radiation of 553.4 KJ/cm^2. Cotton is the staple crop in the study area. Before the land began to be used for agriculture, the main vegetation included sub-shrubs, such as saxioul (Haloxylonammodendron), suaeda dendroides, oleaster, and reaumuria soongorica (Wang et al., 2007).

Under different modes of land use in KADA, the soil can be divided into cultivated land, artificial pasture, woodland, and wasteland (Mao et al., 2007). At present, the economy of the KADA depends mainly on agriculture and agricultural land represents about 70% of the total land in the area. The originally salty groundwater has not been suitable for drinking, industrial or agricultural utilization (Cui et al., 1997), therefore, transfer of water from outside the KADA has and will continue to play a crucial role in meeting domestic, industrial and agricultural water needs. Although groundwater salt concentrations have locally been diluted by the infiltration of transferred surface water to some degree, the bulk of groundwater is in the high salinity range (1–65 g/L) and cannot be utilized for irrigation, hence, there is currently no groundwater abstraction in the area. Due to the extreme climate, the hydrogeological conditions, and the irrigation system, soil salinization has become the limiting factor for sustainable agricultural development in the KADA.

Please cite this article in press as: Han, D., et al. A survey of groundwater levels and hydrogeochemistry in irrigated fields in the Karamay Agricultural Development Area, northwest China: Implications for soil and groundwater salinity resulting from surface water transfer for irrigation. J. Hydrol. (2011), doi:10.1016/j.jhydrol.2011.03.052

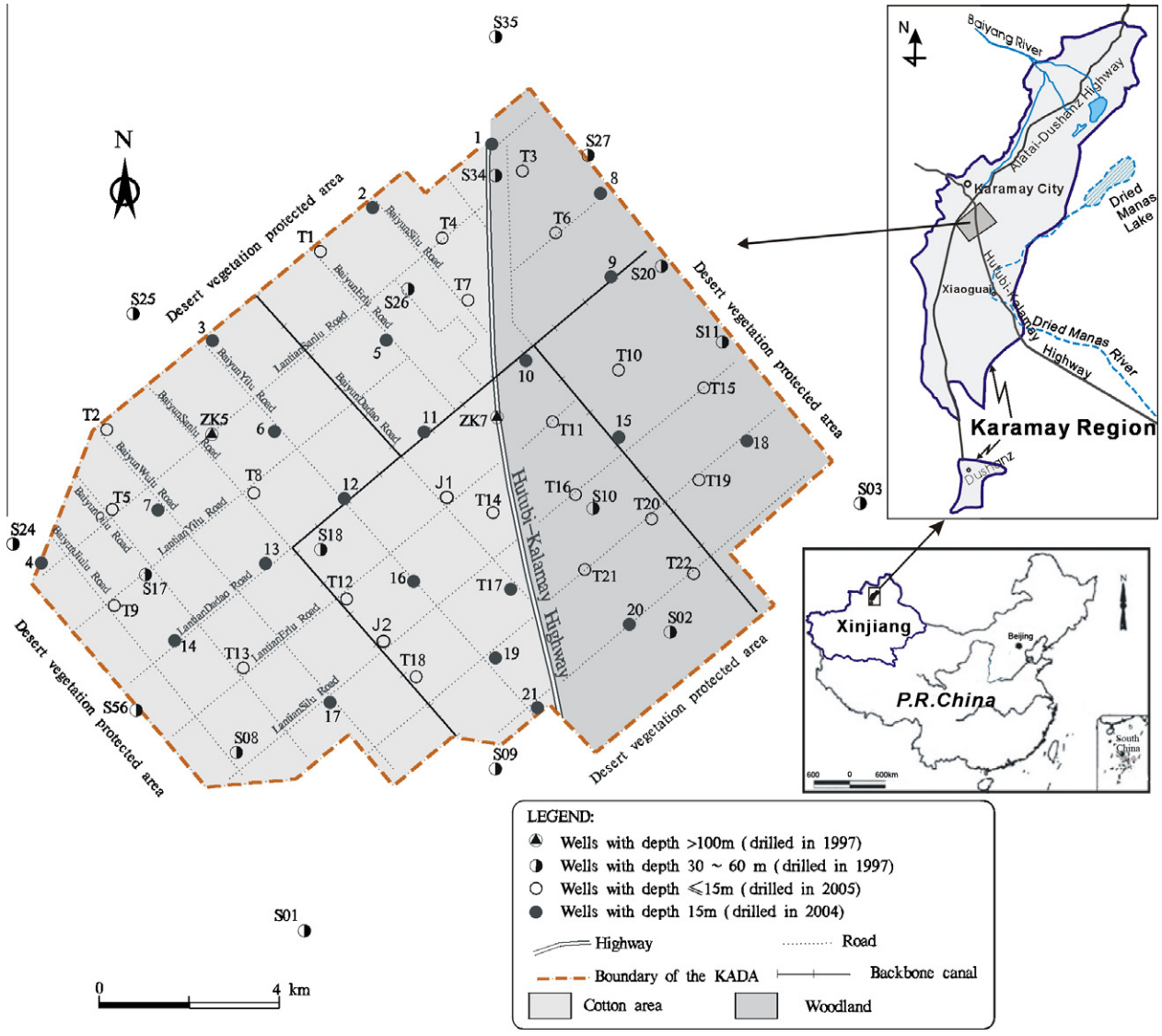

Fig. 2. Location map of Karamay Agricultural Development Area (KADA) and distribution of the monitoring wells. The wells J1 and J2 (<4 m depth), were dug for observing the shallow groundwater table. The well codes refer to both water table measurement and sampling sites. The monitoring wells (ZK5, S17, S25, S35, S34, S18, S24, S26, and 17) have been abandoned since 2005. The line of P–P′ is location of the hydrogeological cross-section in Fig. 3.

3. Hydrogeological setting

The geology and hydraulic properties of rocks in the area have been studied by Cui et al. (1997). The main aquifers in the region are porous Quaternary sediments, which fill the KADA with a thickness ranging from 80 to 100 m in the upstream region to more than 300 m in the downstream regions. These sediments make up an unconfined aquifer, with a depth of <60 m, and a semi-confined aquifer below 60 m depth. The Quaternary sediments consist of alternating layers of sand, gravel and clayey sand derived from the host rocks in the region, including fine sandstone and mudstone of Cretaceous age and clayey conglomerate and mudstone of Neogene age. These rocks are located in the surrounding mountain areas, and comprise the bedrock of the study area. The major geological strata and their characteristics are shown in Table 1. Under the control of the regional topography and hydrogeology, groundwater generally flows from southwest to the north-east, towards the Manas River valley, and ultimately into the (dried) Manas Lake.

The unconfined and semi-confined aquifers exhibit substantial heterogeneity in the study area. In the area enclosed by S10–S11–S3–S2–S10 (Fig. 2), the unconfined aquifer belongs to a paleochannel system and contains sandy gravel. In this area, the aquifer has a hydraulic conductivity of 9.4–57.4 m/d (specific yield 0.16–0.21), and the water is Cl–Na or Cl–Na·Mg-type. In the area enclosed by T1–T2–4–S01–S02–T1 (see Fig. 2), the unconfined aquifer is composed of gravel, silt and fine sand with a hydraulic conductivity of 0.41–0.88 m/d (specific yield 0.08–0.10) and Cl–Na or Cl·SO_4–Na type water. The semi-confined aquifer unit in the area enclosed by T1–S10–S11–S35–T1 (see Fig. 2), is composed of silt, clay and silty clay with the hydraulic conductivity of 0.004–0.944 m/d (specific yield 0.08–0.10) and Cl–Na or Cl–Na·Mg or Cl–Na·Ca-type water (Cui et al., 1997). Generally, below 100 m, groundwater occurs in confined Cretaceous sandstone or mudstone layers, with hydraulic conductivity between 1.26 and 4.6 m/d and Cl–Na or Cl–Na·Ca-type water (Cui et al., 1997). Fig. 3 shows the aquifers, boundary conditions, and distribution of TDS on a schematic hydrogeological cross-section. This study is primarily concerned with hydrogeological characteristics of the shallow aquifer at <60 m depth.

The study area suffers from an acute shortage of surface and groundwater. The rainfall amount is too low, and the neighboring

Please cite this article in press as: Han, D., et al. A survey of groundwater levels and hydrogeochemistry in irrigated fields in the Karamay Agricultural Development Area, northwest China: Implications for soil and groundwater salinity resulting from surface water transfer for irrigation. J. Hydrol. (2011), doi:10.1016/j.jhydrol.2011.03.052

Table 1
Stratigraphic column showing the geological units in the KADA.

Era	Period	Epoch	Symbol	Distribution in the KADA	Lithology description	Thickness
Cenozoic	Quaternary	Holocene	Q_4^{eol}	Mainly in the southeastern area	Aeolian deposit: fine sand and medium-fine sand	2–10 m
		Holocene	Q_4^{pl}	Mountainous regions, of the northwest	Alluvial-diluvial deposit: silt and silty clay in the lower stream of KADA	5–20 m
					Alluvial-diluvial deposit: sand gravel and gravel with clay layers in the upper stream of KADA	0.5–2 m
		Holocene – upper pleistocene	Q_{3-4}^{eol+1}	Middle area	Aeolian and lacustrine deposits: silty clay, silt, clay with the local silty-fine sand lenses	0.5–3 m
		Holocene – upper pleistocene	Q_{3-4}^{eol+a1}	Mainly in the southeastern area	Aeolian and alluvial deposit: sandy gravel, sandy clay, silty clay with the local silty-fine sand	50–60 m
		Upper pleistocene	Q_3^1	Widespread at the middle area	Lacustrine deposits: silt, clay, silty clay with silty-fine sand	20–50 m
		Mid pleistocene	Q_3^{al}	Mainly in the southwestern area	Sandy gravel	1–2 m
	Tertiary	Oligocene	N_2ch (Changjihe group)	Hongshanzui zone, which is located in the southwest KADA	Conglomerate, mudstone	24 m
Mesozoic	Cretaceous	Masst.	K_1t (Tugulu group)	Mountainous areas, northwest of KADA	Fine sandstone and mudstone with fissures	No data

Note: This table was sorted out from the hydrogeological survey report of KADA by Cui et al. (1997).

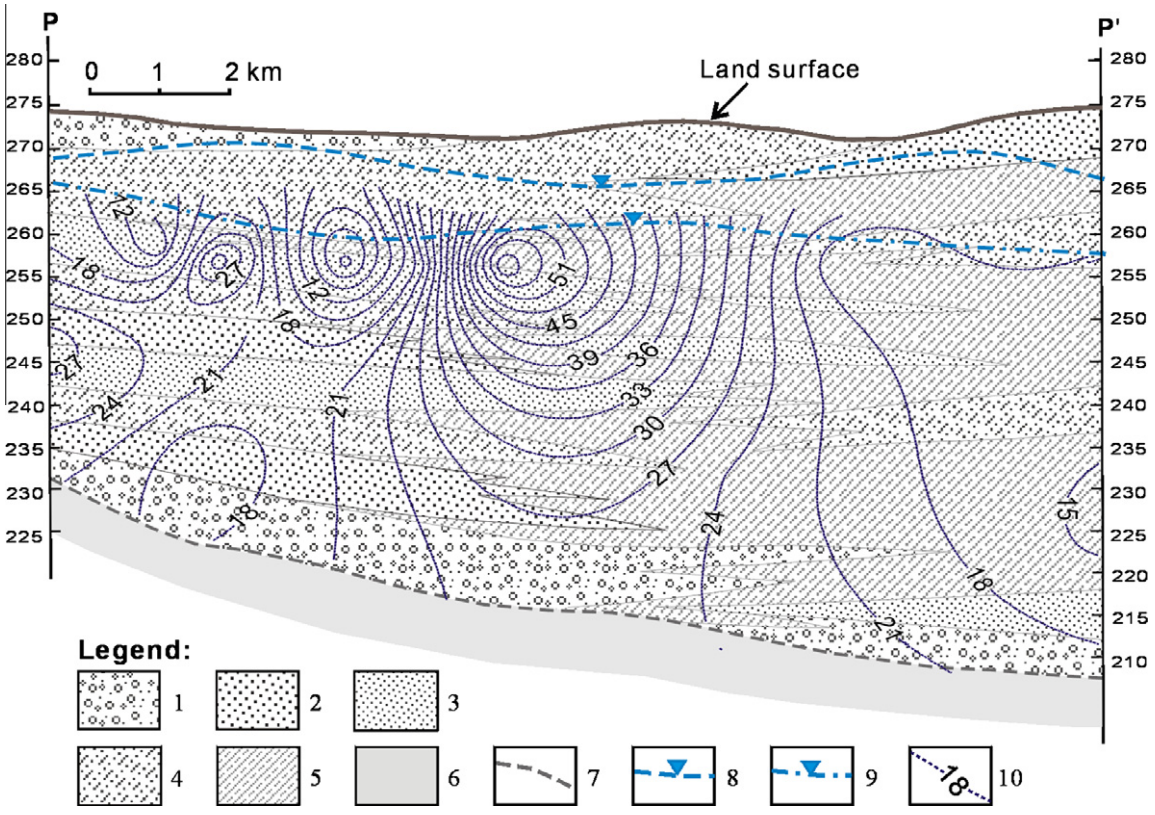

Fig. 3. Hydrogeological cross-section map of P–P′ (for location see Fig. 2) Legend: 1. Sand and gravel; 2. Medium and fine sand; 3. Clayey sand; 4. Sandy clay; 5. Clay; 6. Sandstone inter-bedded with mudstone (Cretaceous); 7. Bedrock boundary; 8. Groundwater table in September 2009; 9. Groundwater table in September 1997; 10. TDS contours (in g/L) with interval of 3 g/L in October 2009.

mountains have too little relief for significant drainage channels to form, except temporarily during rare rainstorm/flood events. The groundwater system in the KADA is recharged via infiltration of precipitation, lateral influx of groundwater from mountain areas, and leakage of agricultural return flow. Groundwater sinks include discharge via evapotranspiration in the shallow soil zone, and outflux of groundwater to downstream areas. Surface soil texture is composed of silty clay loam, silty clay, calcisols, and clay (Wang et al., 2007). The soil salt content is closely associated with the underlying shallow groundwater depth. In KADA, when the groundwater depth reaches 4 m from the ground surface, soil salinization is prone to occur (Cui et al., 1997).

Please cite this article in press as: Han, D., et al. A survey of groundwater levels and hydrogeochemistry in irrigated fields in the Karamay Agricultural Development Area, northwest China: Implications for soil and groundwater salinity resulting from surface water transfer for irrigation. J. Hydrol. (2011), doi:10.1016/j.jhydrol.2011.03.052

4. Materials and methods

Groundwater monitoring bores (total 52) were installed by the Department of Geological Investigation, Design & Research Institute of Water Conservancy & Hydropower in the Xinjiang Uygur Autonomous Region of China. Locations of the 52 wells are shown in Fig. 2. Among these, one deep monitoring well with a depth of 100.5 m and eight shallow monitoring wells with depths between 40 and 55 m were established in 1997; 21 shallow monitoring wells with depths of 15 m were established in 2004 and 22 shallow monitoring wells with depths between 10 and 15 m were established in 2005. Three of these wells are located in the desert, 30 on cotton-producing land, and 19 on the woodland (Fig. 2).

The wells have been in use for various groundwater monitoring purposes in the KADA. Field campaigns were carried out in the KADA for the purpose of investigating groundwater dynamics and water quality changes under the extensive irrigation regime. Water sampling at different aquifer depths was conducted during two periods from August 2008 to October 2009. Data from 52 observation wells has been monitored on a monthly basis by the Agricultural Development office of Kalamay prior to August 2008. Groundwater storage variations were calculated from field measurements of groundwater levels in shallow monitoring wells throughout the aquifer.

Groundwater sampling in the 52 wells was carried out twice, in different seasons (47 samples in August 2008 and 50 samples in October 2009, see Table 2). Samples were collected in cleaned 100 mL polyethylene bottles, tightly capped and stored at 4 °C until analysis. Samples for cation analysis were preserved in acid-washed polyethylene bottles, and acidified to pH < 2 with 6 N HNO_3. Conductivity, pH, and temperature were measured using a portable WM-22EP meter in the field. Alkalinity was determined on filtered samples in the field, by titration with H_2SO_4 (0.25 N). The anions (Cl^-, SO_4^{2-} and NO_3^-) were analyzed using Ion Chromatography (ICS-1500) in the Laboratory of Hydrochemical Composition Analysis, Institute of Geology and Geophysics, Chinese Academy of Sciences. In the Key Laboratory of Water Cycle & Related Land Surface Processes, Institute of Geographic Sciences and Natural Resources Research, China Academy of Sciences, the concentrations of the cations (Na, Mg, Ca and K), together with B and Li were measured using inductively coupled plasma analysis (ICP-OES); and stable isotope ratios (δ^2H and $\delta^{18}O$) were measured using a Finnigan MAT253 mass spectrometer after on-line pyrolysis with a Thermo Finnigan TC/EA. The δ^2H and $\delta^{18}O$ values were measured relative to international standards that were calibrated using V-SMOW (Vienna Standard Mean Ocean Water) and reported in conventional δ (‰) notation. The analytical precision is ±2‰ for δ^2H and ±0.3‰ for $\delta^{18}O$. Major ion and stable isotope data are presented in Table 2.

5. Results and discussion

5.1. Groundwater hydraulics and water table fluctuations

Surface water transfer from the IrtySh River commenced in 2000 with the beginning of land exploitation. Due to the gentle topography and extensive irrigation without any drainage systems, groundwater levels have subsequently risen substantially. Fig. 4 shows the change in the shallow water-table depth distribution and groundwater flow direction from September 1997 to September 2009. Prior to land exploitation, in September 1997, the flow direction was towards the northeast, and the hydraulic gradient of shallow groundwater was 3.1‰ in the upstream area, decreasing in the east of the area to ~0.5‰, possibly reflecting an escalation in the hydraulic conductivity of the aquifer material. It can be seen from Fig. 4 that water table depths in September 1997 ranged from 10 m in the upstream area to 18 m in the downstream area, gradually increasing along the groundwater flow path. These depths are generally too great for significant direct groundwater evaporation to have occurred in 1997. In 2009, the water table was generally much closer to the ground surface (<5 m in most areas) and the groundwater flow directions were far more complex – including a number of local groundwater mounds and depressions (note that the shallow water table was able to be characterized in much greater detail after 2005, with the addition of new shallow monitoring wells).

According to field measurements that investigated the relationship between soil types, soil salts and groundwater table depth, 4 m is the critical water table depth at which shallow groundwater is likely to be affected by continuous evaporation, causing precipitation of salts (Cui et al., 1997). The monitoring data show that the area of land in the KADA where the water table was within 4 m of the ground was 7.4 km^2 in August 2005, increasing to 99.9 km^2 in August 2008, and up to 115.8 km^2 in October 2009. By 2009, the area over which the water table depth was greater than 4 m had decreased to 78.5 km^2 (i.e., it was smaller than the area where the water table was within 4 m of the surface). This indicates a rapid increase in the area exposed to salinization via direct evaporation from the shallow groundwater in the last decade.

Fig. 5 shows the change in water levels over time in some representative wells from the region. Water table depth in the shallow monitoring wells (10–15 m depth) ranged between 1.5 and 12.4 m in May 2005, and 0.9 and 7.9 m in May 2009. Water table depth measured in the wells between 30 and 50 m depth changed from 5.8 to 19.8 m in September 1997, to 5.3 to 17.0 m in September 2009. The variation in water table depths over this period is hence greater in the shallow wells (drilled in 2005) than the deeper pre-existing wells, indicating an attenuation of the influence of irrigation water at depth, which indicates a degree of semi-confined behavior. The response in the deeper wells is however variable, for example, relatively large water level fluctuations are seen in S02 (Fig. 5b), where the aquifer is highly permeable, located in a palaeochannel. The water levels in wells located outside of KADA (e.g. S01, S03 and S09 in Fig. 5b), show minimal variation between 1997 and 2009 (Fig. 5b), indicating that the water table is under dynamic equilibrium and is impacted only to a small degree by the irrigation in the KADA area.

The main growing period for cotton (the staple crop) is from May to October, during which most irrigation occurs, with peak volumes applied during July–August. It can be seen from Fig. 5 that water levels oscillate over the course of a year, partly due to the seasonal influence of the irrigation cycle, with water levels increasing during and immediately after this period. However, this is not always the case, and different water levels in different wells appear to rise or fall at different times of the year. This may be due to different timing in the application of irrigation water and/or different time lags between the irrigation season and the water level rise (e.g. due to differing hydraulic properties across the region). During the irrigation period of 2008 (Fig. 5), the shallow wells (10–15 m depth) are generally characterized by increasing water tables, while the groundwater level in the 30–60 m depth wells is generally stable, with the exception of well S20 (51 m depth, screened in fine sand), which may be directly affected by irrigation leakage from the upper aquifer. At the end of the irrigation period, the groundwater levels tend to drop in many of the 10–15 m depth wells (e.g., well 12, T11, T17, screened in sand and gravel sediments). However, water levels in the 30–60 m depth wells tend to increase from November 2008 to April 2009, indicating a delayed response to the input of irrigation water occurring at depth. Some of the 10–15 m depth wells (e.g., well 1 & T15), show a continuing rise in water levels after the irrigation season. Both of

Please cite this article in press as: Han, D., et al. A survey of groundwater levels and hydrogeochemistry in irrigated fields in the Karamay Agricultural Development Area, northwest China: Implications for soil and groundwater salinity resulting from surface water transfer for irrigation. J. Hydrol. (2011), doi:10.1016/j.jhydrol.2011.03.052

Table 2
Hydrochemical and stable isotopic characteristics of water samples in the KADA.

Well label	Ele. (m a.s.l)	Well depth (m)	Water table Depth(m)	pH	EC (ms/m)	Temp (°C)	K (mg/L)	Ca (mg/L)	Na (mg/L)	Mg (mg/L)	Cl (mg/L)	SO_4 (mg/L)	HCO_3 (mg/L)	B (mg/L)	Si (mg/L)	Sr (mg/L)	TDS (g/L)	$\delta^{18}O$ (‰)	$\delta^{2}H$ (‰)	Water type
Sampled in Oct.2009:																				
1	270.1	15	3	7.54	43.5	13.2	21.7	818.6	9742.0	1991.0	12029.5	9397.5	378.2	3.6	13.0	20.0	34.2	-7.7	-61	Salt
2	271.8	15	1.2	7.61	8.76	14.7	3.9	443.1	1210.0	408.6	1211.0	3189.9	183.0	2.3	4.7	7.7	6.6	-11.8	-87	Brackish
4	274.0	15	4.72	7.24	18.5	12.2	2.3	699.5	3085.0	754.9	3976.6	3836.6	323.3	2.6	13.6	11.7	12.5	-8.9	-75	Salt
5	270.9	15	2.3	8.1	1	13.7	2.0	77.0	112.1	15.2	138.0	128.3	140.3	0.1	3.3	0.5	0.6	-13.0	-90	Fresh
7	271.3	15	4.25	6.93	53	11.3	18.7	838.4	9465.0	2348.0	17180.0	8205.6	384.3	1.7	9.0	23.2	38.2	-8.0	-68	Salt
8	273.1	15	7.35	7.6	17.1	10.2	1.5	491.7	3674.0	557.0	2853.1	5305.7	427.0	3.1	8.9	7.6	13.5	-8.8	-67	Salt
9	275.0	15	5.45	7.35	21	11.6	6.2	584.5	5375.0	913.7	5421.6	6739.0	469.7	3.0	8.4	7.0	19.6	-10.5	-76	Salt
10	270.5	15	2.33	7.5	20.8	13	2.5	579.7	3926.0	674.4	3822.8	6636.3	262.3	2.5	14.4	16.0	16.0	-9.8	-75	Salt
11	272.5	15	7.9	8.13	2.02	10.3	2.7	118.4	250.8	47.4	397.3	212.2	195.2	0.1	3.5	0.9	1.1	-12.3	-88	Brackish
12	271.0	15	5.23	6.97	72.1	11.4	39.1	841.9	15410.0	3487.0	26524.9	12745.6	524.6	8.4	18.4	21.1	59.8	-7.0	-55	Salt
13	271.8	15	2.65	7.85	1.39	13.7	3.6	98.7	177.7	28.7	136.7	182.3	402.6	0.3	7.2	1.1	0.8	-11.9	-94	Fresh
14	272.7	15	1.65	7.65	13.26	13.8	0.0	426.0	2392.0	583.3	2706.7	3319.3	481.9	2.0	9.9	6.3	9.7	-9.9	-66	Brackish
15	275.1	15	4.35	7.52	23.9	11.7	1.0	399.4	3497.0	848.3	8684.9	2394.4	384.3	0.6	5.6	8.8	16.2	-10.5	-79	Salt
16	272.3	15	1.85	7.56	30.5	16.2	6.9	563.5	5709.0	626.8	8852.8	4683.4	219.6	2.5	6.9	12.2	20.6	-8.9	-69	Salt
17	276.6	15	2.1	7.64	28	15.5	9.4	721.8	6669.0	278.7	6751.0	6759.9	219.6	7.3	16.6	11.4	21.3	-11.3	-86	Salt
18	275.4	15	7.55	8.15	1.15	11.2	6.4	75.3	158.0	15.6	150.5	207.3	103.7	0.2	5.3	0.6	0.7	-2.8	-14	Fresh
19	274.2	15	2.1	7.43	47.3	15.2	11.5	934.3	11150.0	552.4	15900.7	3897.3	164.7	4.8	8.7	23.9	32.5	-9.1	-76	Salt
20	278.0	15	4.5	8.02	3.73	12.3	3.6	79.5	698.7	23.3	814.4	506.6	189.1	1.0	7.2	1.3	2.2	-10.2	-73	Brackish
21	277.4	15	7.57	7.21	83.6	11.8	19.3	1638.0	20200.0	1051.0	30015.8	5104.1	298.9	8.7	18.7	54.2	58.2	-8.8	-69	Salt
I_2	Irrigation water			8.11	0.27	13.3	1.2	36.5	21.1	3.2	10.6	53.4	67.1	0.0	2.3	0.2	0.2	-11.9	-87	Fresh
J1	271.7	4	3.82	7.85	20	9.4	5.9	726.0	4565.0	762.6	4008.0	6134.4	115.9	2.8	19.1	15.8	16.7	-10.4	-75	Salt
J2	272.0	3	2.9	7.65	105.4	7.4	45.7	960.6	25170.0	1523.0	38451.3	10824.9	449.0	4.1	3.5	24.5	77.2	-3.0	-44	Salt
S01	284.7	46.5	6.1	10.1	2.49	11.3	3.1	25.8	482.6	4.3	650.3	53.7	207.4	0.3	3.5	0.5	1.3	-5.3	-53	Brackish
S02	276.7	30.3	5.4	7.9	1.52	12.8	3.0	80.2	184.2	48.4	134.3	150.8	555.1	0.6	5.7	2.4	0.9	-11.8	-82	Fresh
S03	275.2	42.8	11.2	9.45	9	10.2	6.0	32.0	1903.0	11.2	2431.5	494.2	311.1	2.7	5.3	2.5	5.0	-11.0	-78	Brackish
S09	277.4	40.6	7.07	9.71	3.85	11.5	6.1	25.4	853.7	4.8	935.2	90.7	452.3	0.6	0.7	0.1	2.1	-8.5	-62	Brackish
S11	276.3	54.7	11.2	8.68	2.65	11.8	3.5	130.2	312.2	110.0	534.4	294.8	97.6	0.5	0.6	1.3	1.4	-11.8	-85	Brackish
S20	277.8	51.0	17.9	7.47	24.1	10.4	20.6	1282.0	3738.0	190.9	8521.9	526.8	36.6	0.5	2.9	33.9	14.3	-10.3	-80	Salt
S27	273.1	41.1	14.6	7.32	55.2	10	73.8	1146.0	11830.0	1542.0	22969.1	5272.8	146.4	10.4	5.1	24.3	42.9	-4.2	-48	Salt
Sampled in Oct.2009:																				
S56	273.9	39	9.95	7.61	45.6	10.9	53.4	781.8	8164.0	1061.0	15876.3	2529.9	30.5	1.9	8.8	13.3	28.5	-6.6	-51	Salt
T1	272.2	15	2.1	7.45	13.19	16	4.2	870.1	1742.0	397.8	3423.2	2226.4	256.2	1.4	8.9	11.9	8.8	-9.3	-74	Brackish
T2	272.0	14.9	3.4	7.61	7.02	13.1	3.3	99.3	444.7	67.5	947.7	345.8	366.0	0.2	3.5	1.3	2.1	-13.0	-90	Brackish
T3	271.6	14.9	2.55	7.71	15.44	12.9	3.6	392.1	3269.0	737.0	2564.0	5208.9	329.4	2.8	10.7	8.6	12.3	-11.1	-79	Salt
T4	270.7	14.8	3.15	7.46	19.98	11.1	1.6	686.3	3890.0	775.9	4067.3	6390.9	335.5	3.1	9.5	13.9	16.0	-11.1	-82	Salt
T6	277.9	15.1	2.35	7.8	6.81	15.1	118.2	267.5	1682.0	340.2	902.2	2202.7	524.6	2.4	11.2	5.2	5.8	-12.7	-88	Brackish
T7	271.9	14.7	2.87	7.51	7.75	13.3	6.4	301.9	660.1	282.7	258.7	2404.4	610.0	1.4	8.1	4.4	4.2	-12.4	-93	Brackish
T8	270.1	10.4	2.15	7.35	20.5	13.7	10.2	486.5	3783.0	874.0	5418.1	4531.3	323.3	1.6	9.9	11.1	15.6	-7.8	-74	Salt
T9	272.4	14.1	1.38	7.56	0.953	14	2.4	78.9	62.5	25.5	30.9	109.0	317.2	0.2	6.5	0.9	0.5	-13.3	-93	Fresh
T11	274.7	14.8	2.4	7.5	33.2	13.1	9.5	616.5	7404.0	1218.0	8836.2	8758.0	372.1	1.6	10.4	12.5	27.3	-10.1	-67	Salt
T12	273.4	15.0	1.17	7.55	22.6	14.9	5.5	465.3	5205.0	453.3	4600.2	6989.0	201.3	3.5	7.8	7.6	17.8	-10.8	-84	Salt
T13	272.4	15.3	1.2	7.09	45.5	15.7	14.5	946.0	9361.0	1121.0	16777.0	3697.1	164.7	1.7	7.7	20.5	32.4	-9.8	-78	Salt
T14	272.0	14.9	1.6	7.41	18.05	13.6	9.5	890.9	3047.0	593.1	5169.7	1951.9	280.6	1.3	14.2	14.7	11.8	-9.5	-73	Salt
T15	275.0	14.6	8.65	7.04	87.5	10.7	34.9	1078.0	19250.0	4700.0	30084.7	10457.3	744.2	2.2	5.8	32.3	66.4	-7.2	-67	Salt
T17	273.2	15.1	1.23	7.34	23.5	14.4	3.8	957.2	4031.0	650.8	7294.8	2611.1	225.7	1.4	8.1	17.0	16.1	-9.1	-78	Salt
T18	274.5	15.2	2.05	7.52	35.8	15.4	9.8	919.6	8633.0	376.3	10946.3	5844.3	134.2	7.6	16.5	16.0	26.8	-11.6	-86	Salt
T19	276.2	14.9	3.5	7.25	33.9	12.5	14.0	626.1	7936.0	872.7	9674.6	3108.3	347.7	2.3	10.6	13.5	22.4	-8.0	-60	Salt
T20	275.1	14.8	2.89	7.2	61.4	13	29.5	860.4	14420.0	1241.0	22146.3	8725.2	488.0	6.3	6.7	20.8	47.7	-5.7	-46	Salt
T21	274.1	14.6	2.14	7.71	8.8	13.6	8.4	285.7	1437.0	147.9	2137.3	1188.0	500.2	0.9	5.5	3.3	5.5	-11.9	-84	Brackish
T22	275.8	13.4	3.18	7.45	7.3	13.9	4.0	813.9	658.0	234.6	1457.6	1927.1	183.0	1.7	8.5	9.0	5.5	-11.2	-80	Brackish
ZK7	272.3	100.5	8.03	8.21	50.9	11.4	82.9	525.6	11390.0	662.6	18570.9	1829.1	268.4	0.2	2.6	11.2	33.2	-7.6	-52	Salt

Please cite this article in press as: Han, D., et al. A survey of groundwater levels and hydrogeochemistry in irrigated fields in the Karamay Agricultural Development Area, northwest China: Implications for soil and groundwater salinity resulting from surface water transfer for irrigation. J. Hydrol. (2011), doi:10.1016/j.jhydrol.2011.03.052

Sampled in Aug.2008:																			
1	270.1	15	4.18	7.45	11.4	13	18.0	816.1	4127.0	785.7	9666.2	4350.2	323.3	2.6	8.9	13.5	19.9	-9.4	-77	Salt
2	271.8	15	2.48	7.81	12.4	16.5	9.0	621.5	1935.0	616.9	2282.9	3902.7	231.8	3.5	6.6	10.7	9.5	-10.8	-87	Brackish
4	274.0	15	5.05	7.33	19.8	12.5	9.0	682.1	3813.0	803.9	4537.1	5302.7	231.8	3.7	7.0	12.7	15.3	-7.4	-72	Salt
5	270.9	15	2.67	7.46	32	14.6	15.3	605.1	7175.0	1277.0	8662.0	8551.3	134.2	5.0	7.4	11.9	26.4	-6.1	-66	Salt
7	271.3	15	5.84	7.46	48.1	11.6	24.5	918.8	9310.0	2169.0	14313.4	8822.7	408.7	1.7	6.9	25.1	35.8	-8.0	-75	Salt
8	273.1	15	7.79	7.38	16.49	11.6	7.9	267.5	3251.0	542.4	2665.2	4933.3	500.2	2.3	7.0	6.1	11.9	-8.2	-69	Salt
9	275.0	15	8.71	7.43	13.4	14.4	8.8	180.0	2970.0	366.8	2591.3	3069.3	500.2	2.6	8.1	7.0	9.4	-11.4	-85	Brackish
10	270.5	15	2.83	7.5	14.4	14.3	8.8	549.3	3439.0	660.9	2688.8	5874.0	280.6	3.0	7.7	10.0	13.4	-9.9	-82	Salt
11	272.5	15	8.74	7.49	53.6	11.6	37.4	1079.0	10420.0	2224.0	19885.3	6604.1	231.8	4.6	6.1	29.8	40.4	-7.7	-70	Salt
12	271.0	15	5.49	7.27	79.1	12.1	47.8	864.5	17580.0	4103.0	26636.6	15416.4	561.2	8.7	6.7	23.3	64.9	-6.4	-63	Salt
13	271.8	15	1.76	7.73	3.1	17.2	5.9	112.2	346.8	76.0	264.3	584.4	414.8	0.6	8.4	2.9	1.6	-11.6	-94	Brackish
14	272.7	15	4.21	7.19	50.2	12.2	34.5	770.2	10950.0	2655.0	13898.4	12547.8	463.6	4.2	6.3	16.8	41.1	-4.7	-54	Salt
15	275.1	15	4.5	6.95	23.7	11.7	17.6	855.9	3930.0	1242.0	6598.8	4350.1	420.9	1.5	8.9	13.6	17.2	-10.4	-86	Salt
16	272.3	15	0.64	7.52	41.3	25.9	22.9	919.5	8843.0	1025.0	12834.9	6643.5	201.3	3.4	6.6	19.6	30.4	-5.5	-51	Salt
17	276.6	15	1.77	7.68	15.3	19.8	9.9	274.8	3295.0	118.9	2897.6	2933.5	323.3	4.4	5.8	4.5	9.7	-5.6	-52	Brackish
18	275.4	15	4.68	7.92	12.1	12.1	8.7	224.1	2702.0	220.7	1918.4	2913.7	347.7	2.4	8.3	4.7	8.5	-11.0	-86	Brackish
19	274.2	15	4.5	7.52	37.2	13.8	13.7	818.7	8266.0	422.6	12568.0	3308.5	201.3	4.3	7.6	21.5	25.5	-9.8	-77	Salt
20	278.0	15	5.45	8.05	4.1	15.3	30.4	109.6	147.8	35.9	160.9	220.3	335.5	0.2	10.0	1.0	0.9	-7.9	-60	Fresh
S01	284.7	46.5	6.05	9.9	2.4	12.8	3.3	7.4	473.9	1.2	620.8	39.9	219.6	0.6	0.5	0.4	1.3	-7.4	-60	Brackish
S02	276.7	30.3	6.42	7.96	1.2	13.6	17.4	41.8	279.0	42.5	198.7	26.5	591.7	0.8	4.0	1.7	1.0	-11.7	-94	Brackish
S03	275.2	42.8	12.44	9.68	4.7	11.4	7.2	15.8	1983.0	4.5	2614.0	482.2	298.9	3.0	0.9	2.8	5.3	-10.7	-76	Brackish
S09	277.4	40.6	7.27	9.97	3.9	14.5	6.4	3.0	761.0	0.3	607.6	109.4	542.9	0.6	0.4	0.0	1.8	-9.2	-73	Brackish
S11	276.3	54.7	13.54	8.57	31.8	14.3	37.0	673.3	13530.0	2728.0	26078.3	9205.1	207.4	1.9	2.2	13.9	52.4	-6.0	-59	Salt
S20	277.8	51.0	18.55	6.74	60.8	12.2	61.9	5105.0	10370.0	586.3	22917.2	1453.2	201.3	2.6	4.7	117.1	40.6	-7.2	-70	Salt
S27	273.1	41.1	14.52	7.62	54.8	12.4	77.6	1168.0	11690.0	1523.0	18434.9	6387.9	591.7	10.8	3.4	23.7	39.6	-4.5	-51	Salt
S56	273.9	39.0	10.725	7.25	45.6	15.6	55.9	1095.0	9080.0	1200.0	15690.1	3530.4	335.5	2.6	3.3	20.6	30.8	-6.2	-61	Salt
T1	272.2	15.0	1.74	7.36	15.1	18.3	11.5	1310.0	2025.0	531.2	4333.2	2287.2	225.7	1.4	7.6	16.4	10.6	-7.8	-70	Salt
T2	272.0	14.9	2.78	7.68	39.2	14.6	31.6	836.2	8527.0	1508.0	13726.7	5906.6	378.2	2.1	8.0	21.3	30.7	-9.9	-78	Salt
T3	271.6	14.9	2.7	8.17	5.2	15.1	7.4	342.1	1721.0	438.9	1608.4	3289.6	366.0	2.1	6.9	6.6	7.6	-10.6	-84	Brackish
T4	270.7	14.8	3.48	7.14	21.1	12.1	9.8	769.3	3903.0	916.1	5445.4	4848.9	475.8	2.9	8.5	16.4	16.1	-9.9	-81	Salt
T5	273.6	8.7	6.73	8.14	1	12.2	3.9	42.5	211.2	26.6	57.3	108.1	494.1	0.9	5.1	0.7	0.7	-11.5	-92	Fresh
T6	277.9	15.1	2.39	7.53	7.4	17	7.8	300.7	1250.0	330.3	1231.0	2609.3	207.4	1.7	8.3	5.8	5.8	-11.7	-95	Brackish
T8	270.1	10.4	1.61	7.81	17.7	14.6	15.2	367.9	3538.0	697.1	4204.5	3690.7	298.9	2.0	7.6	8.6	12.9	-9.7	-75	Salt
T9	272.4	14.1	3.86	7.36	5.9	12.9	9.5	178.1	1132.0	129.1	665.9	1493.2	500.2	1.7	8.8	3.1	3.9	-12.2	-95	Brackish
T11	274.7	14.8	2.68	7.78	17.9	14.7	11.4	523.9	4424.0	559.0	2101.4	7872.4	353.8	1.7	8.7	9.0	15.7	-11.1	-87	Salt
T12	273.4	15.0	2	7.85	22.6	18.1	11.1	408.7	5226.0	435.2	4416.7	6273.3	170.8	3.4	6.3	8.8	16.9	-11.1	-88	Salt
T13	272.4	15.3	0.86	7.14	52.7	23.6	17.7	880.3	10990.0	985.5	15180.8	6697.5	134.2	2.1	6.6	18.9	34.8	-9.2	-83	Salt
T14	272.0	14.9	1.77	7.58	33.5	13.1	14.8	1516.0	5537.0	1093.0	11150.8	3595.3	292.8	1.9	7.8	28.4	23.1	-9.4	-79	Salt
T15	275.0	14.6	9.27	7.22	88.3	12.5	40.6	1015.0	18250.0	4443.0	33212.7	12774.8	677.1	2.8	8.2	24.5	70.1	-7.4	-64	Salt
T16	275.8	10.9	2.63	7.07	38.3	13.3	19.2	1269.0	7665.0	1349.0	12470.5	4815.2	408.7	2.5	6.7	23.3	28.5	-9.8	-83	Salt
T17	273.2	15.1	0.55	7.71	19.9	21.5	6.8	926.0	3759.0	583.1	5416.7	3954.5	244.0	1.7	6.6	14.9	15.2	-9.9	-84	Salt
T18	274.5	15.2	2.37	7.11	69.9	15	15.4	1030.0	14170.0	846.3	25037.8	7817.0	128.1	6.0	7.3	24.2	49.0	-8.7	-76	Salt
T19	276.2	14.9	4.57	7.63	29	12.4	27.1	676.2	6148.0	710.8	7486.5	5783.6	329.4	3.6	8.2	13.0	21.3	-10.3	-82	Salt
T20	275.1	14.8	4.25	7.62	16.5	12.7	16.2	407.2	3550.0	406.1	3161.9	4531.5	201.3	3.4	11.8	8.7	12.2	-11.0	-90	Salt
T21	274.1	14.6	2.09	7.4	18.7	15.7	65.1	839.0	3403.0	370.7	4844.1	2595.3	201.3	1.1	9.1	8.6	12.2	-10.3	-84	Salt
T22	275.8	13.4	6.15	7.63	23.7	13.6	10.9	762.0	7248.0	312.4	8984.7	4694.3	317.2	5.4	8.2	19.0	22.2	-8.9	-73	Salt
ZK7	272.3	100.5	9.06	8.64	47.5	12.5	89.1	233.2	10940.0	660.3	17750.2	1433.8	408.7	0.3	2.2	4.5	31.3	-7.2	-62	Salt

Please cite this article in press as: Han, D., et al. A survey of groundwater levels and hydrogeochemistry in irrigated fields in the Karamay Agricultural Development Area, northwest China: Implications for soil and groundwater salinity resulting from surface water transfer for irrigation. J. Hydrol. (2011), doi:10.1016/j.jhydrol.2011.03.052

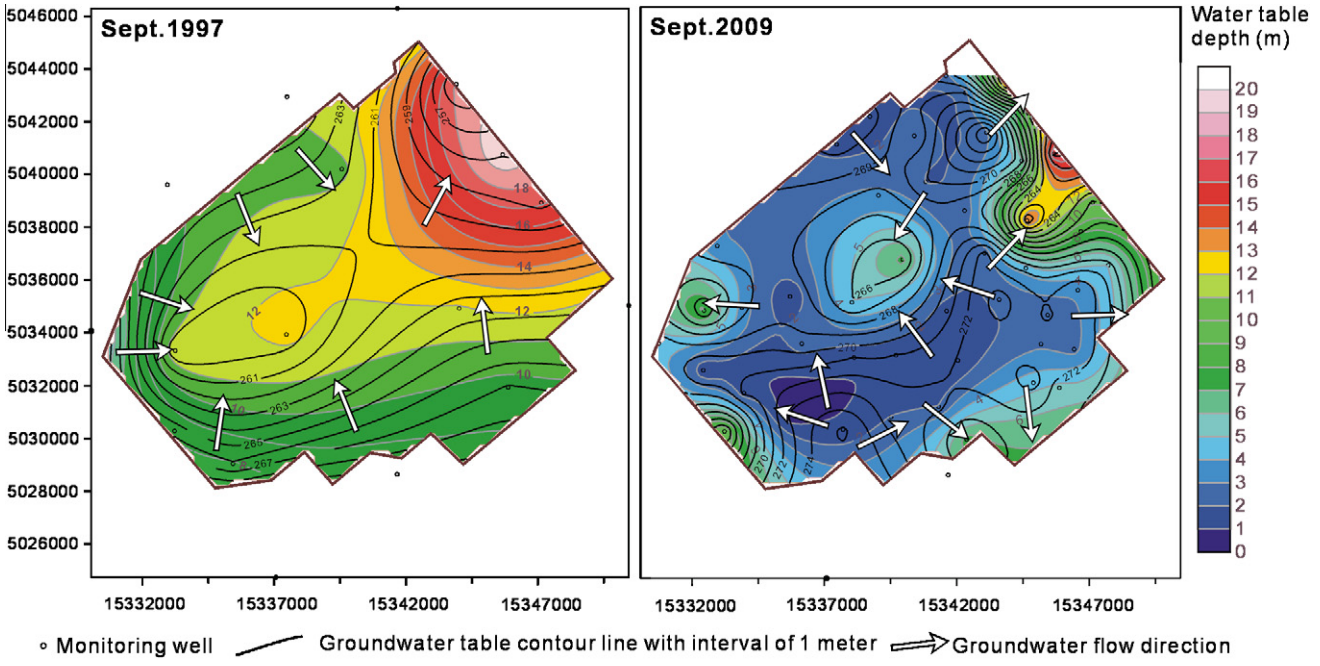

Fig. 4. Water table distribution in the KADA shallow aquifer in September 1997 and September 2009, respectively. The color scale represents water table depth (m).

these wells are screened in silt or fine sands, hence, they appear to exhibit a delayed response to leakage from irrigation return flow. The increasing groundwater level in the deep well ZK7 (100.5 m depth, screened in 6 m thickness of sandstone) suggests that the groundwater level in the deep confined aquifer is also increasing and is likely influenced by downward leakage from the shallow aquifer.

Fig. 6 shows the spatial change (amplitude and sign) in water table depth from the end of the irrigation season (Oct) to the beginning of the season in the following year (May), for 2005, 2008 and 2009. The amplitude of the change was highest in 2005, ranging from −4.5 m to +5.1 m, while the amplitude was lesser in 2008 and 2009, ranging from −2.9 m to +2.6 m and −3.0 m to +1.9 m, respectively. The attenuation of the seasonal fluctuation in water tables in the most recent period is an indication that water saving plans, implemented in 2006, may have started to play a role in regulating the shallow water table. However, overall, the water levels continued to follow an increasing trend over 2008 and 2009.

5.2. Groundwater storage

Groundwater storage is an important component of the hydrologic cycle, which must be accounted for when attempting to quantify groundwater recharge, lateral movement, and evapotranspiration. Groundwater storage changes were estimated for the KADA area on the basis of measurement of shallow groundwater levels (e.g. Healy and Cook, 2002). Annual groundwater level changes were calculated from September 1997 through to September 2009. Monthly or seasonally averaged periods were not used because the water levels were measured manually and data were not available for every month.

Groundwater level changes were converted to groundwater storage (ΔS) by multiplying water level changes by the area and specific yield:

$$\Delta S = \Delta h \cdot A \cdot S_y \quad (1)$$

where Δh is the average groundwater level change across the study area for the period; A is the area of the study area; and S_y is the specific yield. Specific yield in the study area, based on 23 pumping tests (Cui et al., 1997), ranges from 0.05 to 0.16. In this study, an area-weighted average specified yield 0.12 was used to calculate the groundwater storage change. A single representative value of the groundwater level change was calculated as following: First, the study was divided into a mesh of 2 × 2 km cells, and groundwater level changes were calculated at locations where monitoring data in the two time periods were available (Fig. 7a). Then, each cell of the mesh was assigned a mean value for the water level change based on all measurements within it (Fig. 7b). Finally, an area-weighted average was calculated from the cells with data available in it to represent the average groundwater level change (Δh) across the study area. Fig. 8 shows the accumulated total storage variation since September 1997, based on this method. The accumulated total storage is approximately +150 million cubic meters of water from September 1997 to September 2009 (150.04×10^6 m^3), with the average change in groundwater table being +6.9 m (Table 3). The average yearly net groundwater recharge for the KADA over the 12 year period is thus approximately 12.5×10^6 cubic meters.

5.3. Water budget of the aquifer

In terms of the groundwater budget for the KADA, changes in groundwater storage can be attributed to recharge and subsurface lateral in-flow minus evaporation and subsurface lateral outflow (groundwater discharge to the paleo-riverbed of the now dried Manas River). There is no groundwater extraction in this area.

The budget can be written as:

$$\Delta S_{gw} = Q_p + Q_i + Q_{lr} - ET_{gw} - Q_{ld} \quad (2)$$

ΔS_{gw} is the change in subsurface storage, Q_p is precipitation infiltration, Q_i irrigation infiltration, Q_{lr} the lateral groundwater recharge, ET_{gw} evapotranspiration and Q_{ld} is the lateral groundwater discharge; all terms are expressed as rates (e.g., m^3/a).

Accurate estimation of groundwater recharge is extremely important for proper management of groundwater systems, particularly in arid regions (de Vries and Simmers, 2002). The three major recharge terms in the overall water balance are estimated below. Precipitation infiltration can be calculated by the equation:

Please cite this article in press as: Han, D., et al. A survey of groundwater levels and hydrogeochemistry in irrigated fields in the Karamay Agricultural Development Area, northwest China: Implications for soil and groundwater salinity resulting from surface water transfer for irrigation. J. Hydrol. (2011), doi:10.1016/j.jhydrol.2011.03.052

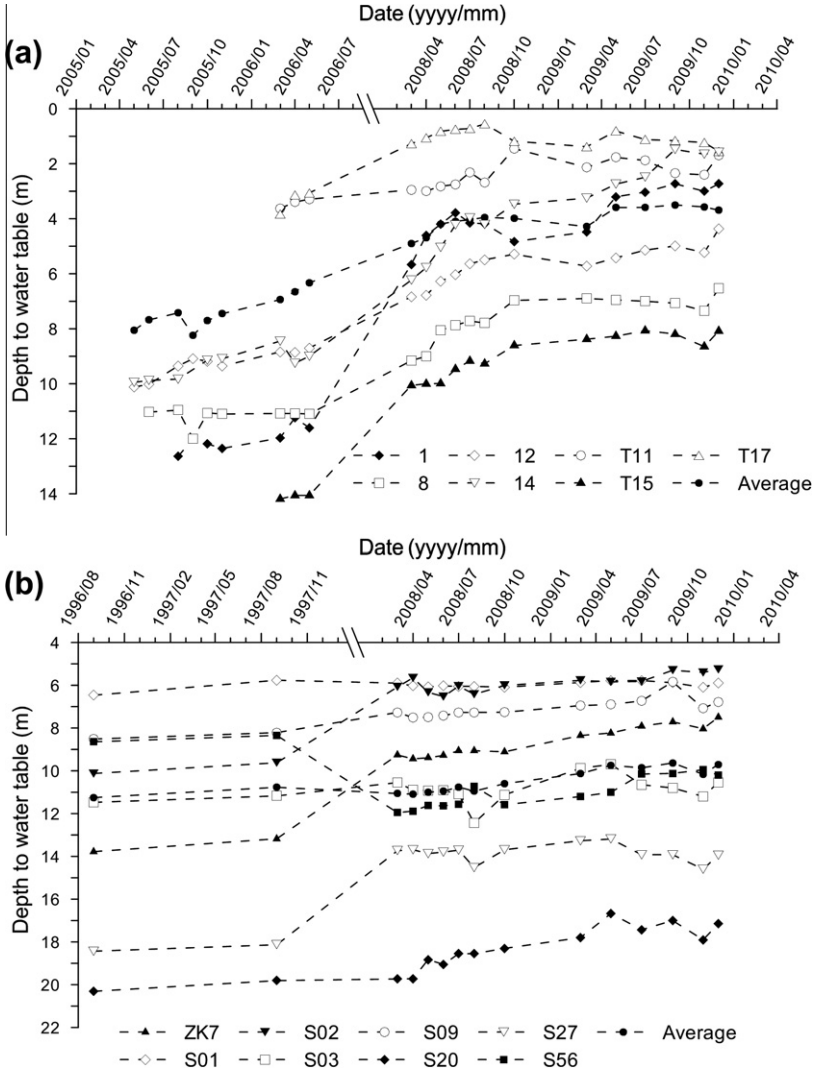

Fig. 5. Variation in depth to groundwater table from typical wells at the time of monitoring, (a) wells with depths of 10–15 m and (b) wells with depths of 30–50 m, with the exception of ZK7 (depth of 100.5 m).

$$Q_p = R_e \cdot F_1 \cdot \alpha_1 \cdot 1000 \tag{3}$$

where R_e average annual effective rainfall (77.6 mm), F_1 catchment area (161.4 km^2 with water table depth less than 6.5 m, which is the water table extinction depth for rainfall infiltration, unpublished report "Groundwater resources of Xinjiang Uygur Autonomous Region in 1985"), α_1-rainfall infiltration coefficient (0.05 for silt and silty clay in this study area), therefore, $Q_p = 0.63 \times 10^6$ m^3/a.

According to the field investigation, the main irrigation mode is flood irrigation. This recharge item can be calculated by the equation:

$$Q_i = F_2 \cdot R_i \cdot \alpha_2 \tag{4}$$

where F_2-irrigation area ($194.3 \times 0.9 = 174.9$ km^2, subtracting the area of channels and roads), R_i-irrigation ration (762.03×10^3 m^3/km^2 a, which is annual average value according to the statistical records from 2001 to 2008), α_2-irrigation infiltration coefficient (0.13). On this basis, $Q_i = 17.3 \times 10^6$ m^3/a.

Lateral groundwater recharge in the study area mainly consists of pore water recharge from the piedmont plain in the southwest and northwestern mountainous areas. The hydraulic features of the boundary areas around KADA such as thickness, length, and corresponding hydraulic conductivity of permeable layers in different boundary sections, can be estimated on the basis of the hydrogeological investigation of KADA by Cui et al. (1997). Using Darcy's Law and the distribution of water tables and groundwater gradients, the lateral groundwater recharge in this area can be calculated:

$$Q_{lr} = \sum_{i=1}^{i=n} k_i I_i H_i \mathrm{B_i} \sin\alpha \tag{5}$$

where k-hydraulic conductivity (m/d), I-hydraulic gradient, H-aquifer thickness (m), B-breadth of flow cross-section (km), α-included angle (°) between groundwater flow direction and flow cross-section. The hydraulic sections of the boundary are shown in Fig. 9, which is drawn according to the mean values based on monitoring data of shallow groundwater table from September 1997 to September 2009. The parameters selected (on the basis of Cui et al., 1997) are shown in Table 4. According to this method, $Q_{lr} = 0.73 \times 10^6$ m^3/a.

Lateral groundwater discharge also can be calculated using:

$$Q_{ld} = \sum_{i=1}^{i=n} k_i I_i H_i \mathrm{B_i} \sin\alpha \tag{6}$$

where the terms in the equation are the same as for (5). The associated parameters are shown in Table 3. The calculated value is: $Q_{ld} = 0.20 \times 10^6$ m^3/a.

Please cite this article in press as: Han, D., et al. A survey of groundwater levels and hydrogeochemistry in irrigated fields in the Karamay Agricultural Development Area, northwest China: Implications for soil and groundwater salinity resulting from surface water transfer for irrigation. J. Hydrol. (2011), doi:10.1016/j.jhydrol.2011.03.052

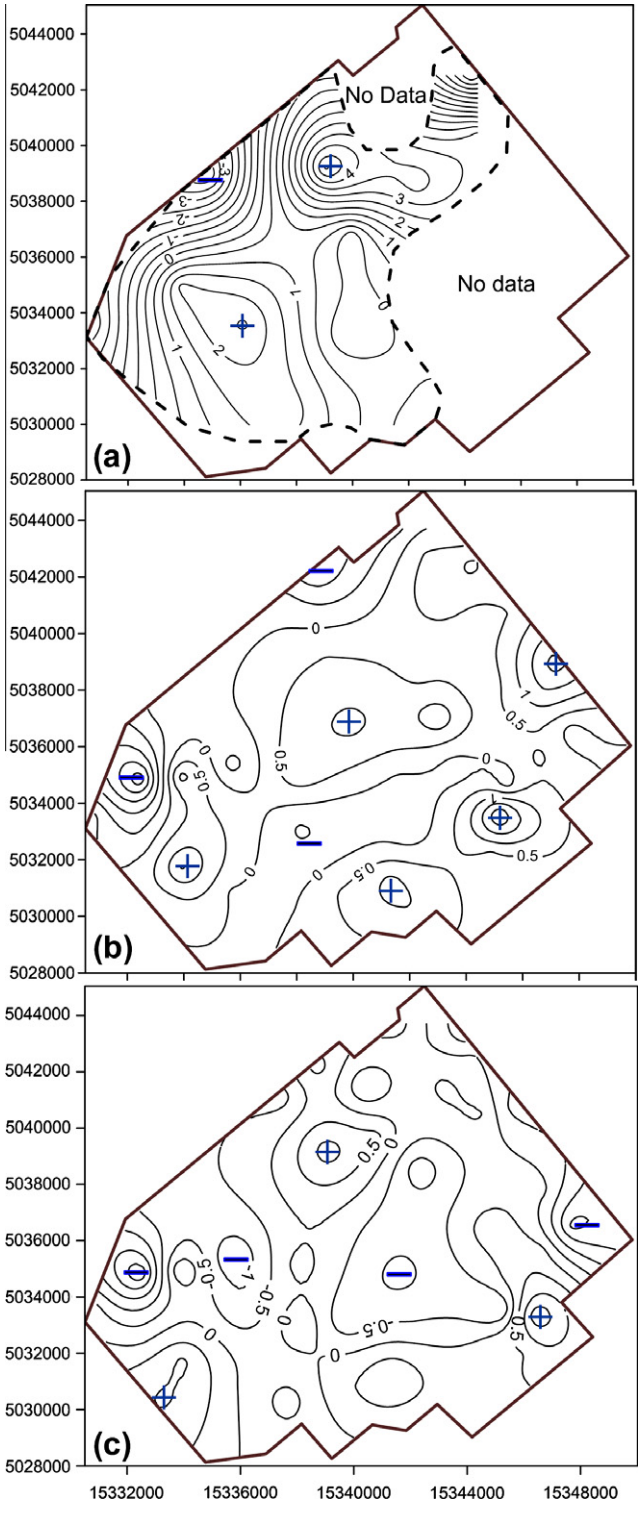

Fig. 6. Amplitude distribution of shallow groundwater table change during the main growing period for cotton. (a) Shallow groundwater table in October 2005 minus that in May 2005; (b) Shallow groundwater table in October 2008 minus May 2008; (c) Shallow groundwater table in October 2009 minus May 2009. Symbols, "+" and "−", denote increasing trend and decreasing trend in water table depth respectively.

Measurements of actual ET_{gw}, an important term in the water balance, are complicated. According to the hydrological balance Eq. (1), the evapotranspiration from groundwater can be calculated as $ET_{gw} = Q_p + Q_i + Q_{lr} - Q_{ld} - \Delta S_{gw}$. Therefore, on the basis of the annual change in storage calculated using (1), it is estimated that $ET_{gw} = 5.96 \times 10^6$ m^3/a.

The results of water budget of the aquifer show that the irrigation infiltration occupied over 90% of the total recharge of the groundwater flow system in KADA. In general, the main source of recharge is irrigation infiltration and the main method of discharge is evapotranspiration. The average yearly net groundwater recharge for the entire KADA from September 1997 to September 2009, is approximately 12.5×10^6 m^3/a.

5.4. Hydrochemical and stable isotopic signatures of groundwater

Stable isotopic and other geochemical tracers can be adopted to investigate groundwater recharge processes, mixing and flow dynamics in arid regions (e.g. Edmunds et al., 2006; Stadler et al., 2010). In the KADA, no such information has been previously reported.

5.4.1. Groundwater hydrochemical composition

Hydrogeochemical analysis of groundwater was used to help delineate the origins of salinity and characterize the evolution of groundwater quality. Overall, groundwater ranges in TDS from 0.5 to 66.4 g/L with a mean and a standard deviation of 14.8–15.9 g/L, respectively. Groundwater in the majority of the shallow alluvial aquifer has salinities ranging from ~10 to 35 g/L. In terms of salinity, groundwater can be classed into three types: fresh, brackish and salt water, with TDS values of <1 g/L, 1–10 g/L, and 10–100 g/L, respectively (Fetter, 1994; Nonner, 2006). Table 1 shows the major constituents of the groundwater, in addition to the TDS, field electrical conductivity (EC), pH, and temperature. Fig. 10a shows the regional distribution of TDS and hydrochemical type in the KADA as of October 2009.

The concentrations of major ions in the groundwater were notably higher than those in the irrigation water (Table 2). The chemical composition of the irrigation water (from the river) was $HCO_3{\cdot}SO_4$–Ca·Na type with TDS of 0.2 g/L. NO_3^- concentration of the shallow groundwater varies widely from 7.8 mg/L (well 5) to ~701.4 (well T16) mg/L, with mean value of 270 mg/L. The wells located out of the KADA (e.g. S01 and S02) have lower NO_3^- concentrations (10.7 mg/L and 52.3 mg/L, respectively), however these are still high compared to typical natural backgrounds, and are above the recommended allowable drinking water level (10 mg/L) of the World Health Organization (World Health Organisation, 1984). The elevated nitrate concentrations in this groundwater are typical of the arid deserts of western China, where nitrogen fixation by bacteria and/or vegetation occurs, and the highly aerobic conditions limit de-nitrification, resulting in the accumulation of significant concentrations of natural nitrate in shallow groundwater (Gates et al., 2008).

The Piper plot of major ion compositions (Fig. 11) shows the variation in groundwater hydrochemistry in the area. Groundwater in the southeast of KADA, such as well S02 and S03, is $HCO_3{\cdot}$Na·Ca or $Cl{\cdot}SO_4$–Na type with TDS of less than 10 g/L (fresh or brackish). In the central KADA, the gentle topography and fine sediments lead to limited groundwater flow and, with exception of well eight, groundwater table depths are mostly less than 4 m from the ground. These conditions are highly favorable to evaporation, hence the water in this area is 'salt water', with TDS of more than 20 g/L, and it is generally Cl–Na or Cl–Na·Ca type. In the north of KADA, the groundwater is also salt water, and is $Cl{\cdot}SO_4$–Na and Cl–Na type. In the southwest KADA, groundwater from 10–15 m depth is generally $Cl{\cdot}SO_4$–Na type, with TDS values from ~10 to 25 g/l, while that from 30–60 m and 100 m depth is generally Cl–Na type and has TDS values from (~1 to 30 g/L). Overall, the freshest groundwater (e.g. TDS <1 g/L, e.g. in the southeast of the area) has higher proporations of HCO_3, SO_4, Ca and Mg, while the more

Please cite this article in press as: Han, D., et al. A survey of groundwater levels and hydrogeochemistry in irrigated fields in the Karamay Agricultural Development Area, northwest China: Implications for soil and groundwater salinity resulting from surface water transfer for irrigation. J. Hydrol. (2011), doi:10.1016/j.jhydrol.2011.03.052

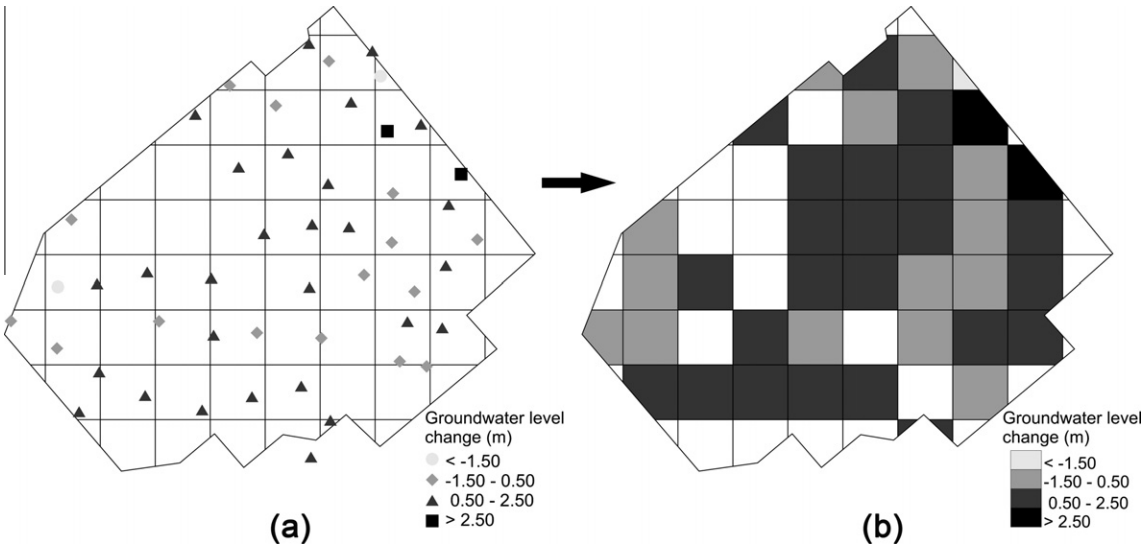

Fig. 7. Illustration of process used to calculate average groundwater change across the study area: (a) example of groundwater level changes between September 2008–September 2009, and (b) groundwater level changes were spatially averaged over a 2 × 2 km mesh. There is no data in the white sections of map b.

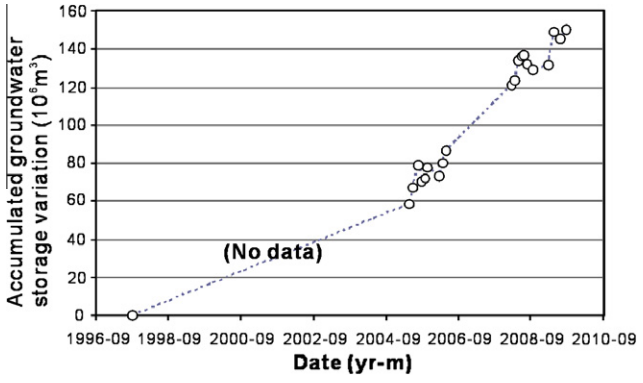

Fig. 8. Cumulative change in shallow groundwater storage from September 1997 to September 2009.

saline samples are Cl–Na dominated. Most groundwater is not suitable for agricultural irrigation, being too saline. Wells located out of the KADA, such as S01, S03, and S09, where irrigation has not occurred, are also generally Cl–Na dominated and are still brackish (TDS from 1 to 5 g/L), suggesting that the regional shallow groundwater is naturally saline due to evapotranspiration during recharge, and/or transpiration from the groundwater table.

Fig. 12 shows the variation of groundwater TDS concentrations from selected wells throughout the seven periods over which TDS was recorded. In recent years it can be seen that some wells with 15 m depth (such as 2, 4, and 7), located upstream of the KADA, were characterized by stable TDS contents. In the southeast of KADA, wells with 15 m depth (such as 1, and 19) showed increasing TDS concentrations. In the center or on the edge of KADA, TDS decreased in wells 15 and 20, while a sharp increase occurred in well of 12, which is screened in thick sandy clay and clay (K = 0.037 m/d). Generally, the TDS of groundwater shows complex variation over time due to the heterogenous aquifer and the transient changes resulting from dilution by fresh irrigation water and subsequent evapo-concentration. The wells with 30–60 m depth generally showed decreasing TDS concentrations in recent years compared with September 1997. The wells located on the southern edge of KADA, such as S01, S02, S03, and S09, show slight decreases in TDS concentrations, while S27, located at the northeast of KADA, displayed a slight increase in TDS concentrations over the period.

Table 3
Calculated change in shallow groundwater storage in KADA during different periods.

Period (m/yyyy)	Average change in groundwater level (m)	Storage change (million m^3)
9/1997–5/2005	3.00	58.2
5/2005–5/2006	1.20	28.0
5/2006–5/2008	2.05	47.8
5/2008–5/2009	0.64	14.9
5/2009–9/2009	0.05	1.2
Total amount	6.94	150.1

The TDS of shallow groundwater in September 1997 ranged between 1.6 and 56.7 g/L, while the area of shallow groundwater with TDS less than 10 g/L was 48.2 km^2. In August 2005, the range in TDS was from 2.6–53.2 g/L and the area <10 g/L was 32.9 km^2; in August 2008, TDS ranged from 0.7 g/L to 70.1 g/L and the area <10 g/L was 26.8 km^2; while in October 2009, the shallow TDS ranged from 0.5 to 66.4 g/L and the area was 45.5 km^2. The decrease in TDS between August 2008 and October 2009 may also in part reflect the slight decrease in water tables, reducing phreatic evaporation over this period, which may be a result of water-saving measures beginning to have an effect in the area. Comparison of the water-table change amplitudes from September 1997 to October 2009 (Fig. 10b) and the TDS contour map (Fig. 10a) shows that TDS is commonly lower in areas where the water table fluctuations are higher. The TDS of shallow groundwater is below 15 g/L in the locations with the biggest water table changes have occurred over time (>10 m). This may relate to the permeability and infiltration rates, e.g. evaporation from the shallow groundwater would be limited in areas where water infiltrates to deep levels relatively quickly, and the shallow water table drops off rapidly after the irrigation season. Alternatively, dilution of the saline local shallow groundwater with fresher irrigation water may be relatively large in these palaeochannel areas, as the aquifer is more conductive.

5.4.2. Saturation index values, sodium adsorption rates and major ion rations

SI values of calcite and dolomite were calculated for the groundwater samples from October 2009 as shown in Figs. 13a–c. Most waters are at or above calcite and dolomite saturation. In general,

Please cite this article in press as: Han, D., et al. A survey of groundwater levels and hydrogeochemistry in irrigated fields in the Karamay Agricultural Development Area, northwest China: Implications for soil and groundwater salinity resulting from surface water transfer for irrigation. J. Hydrol. (2011), doi:10.1016/j.jhydrol.2011.03.052

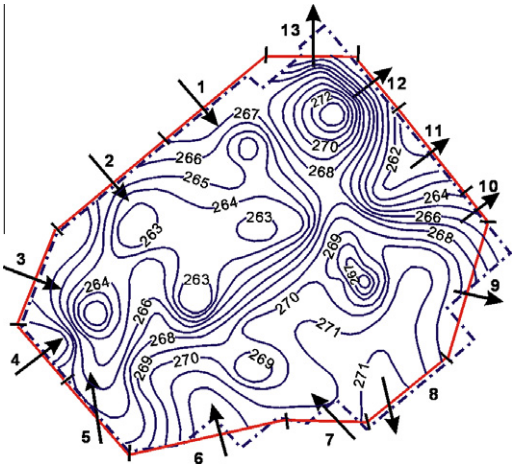

Fig. 9. Subsection of in-flow and out-flow hydraulic boundaries around KADA. Arrows point the lateral groundwater flow directions. This map is drawn according to the mean water table derived from monitoring data during September 1997–September 2009.

the mean SI for gypsum fluctuates around equilibrium (SI = 0) in the salt groundwater (TDS > 10 g/L), while the negative gypsum indices in fresh and brackish waters with TDS < 10 g/L indicate under saturation. Gypsum and/or calcite precipitation occurring as groundwater becomes more saline and reaches super-saturation with respect to these minerals, is likely responsible for the trend towards Na and Cl-dominated groundwater with increasing salinities (e.g. Ca, HCO_3 and SO_4 are removed).

The sodium adsorption rate (SAR) in the groundwater was calculated using Ca^{2+}, Mg^{2+}, Na^+ concentrations as defined by Chappell et al. (1999):

$$SAR = Na^+/SQRT[(Ca^{2+} + Mg^{2+})/2]$$

where all concentrations are in mmol/L. The SAR values of groundwater sampled in October 2009 are summarized in Fig. 13d. Based on these values, groundwater from only a small number of wells fall within the "suitable for irrigation" class (SAR values < 10). Thus, the use of groundwater for irrigation in the region would be likely to increase soil salinity and affect crop yields.

The molar ratios of major cation/Cl concentrations can reflect hydrogeochemical evolution in arid and semi-arid conditions (Herczeg and Edmunds, 2000). The trends in K/Cl, Ca/Cl, Mg/Cl and Na/Cl vs. Cl (Fig. 14) are all similar to one another, with high ratios in the low salinity water, and lower ratios in the more saline groundwater. Weathering of K-feldspar and the Ca and Na end-members of plagioclase by incongruent reactions (e.g. $2NaAlSi_3O_8 + 9H_2O + 2H_2O + 2CO_2 = Al_2Si_5O_5(OH)_4 + 2Na^+ + 2HCO_3^- + 4H_2SiO_4$) can explain the relatively high Na/Cl, K/Cl and Ca/Cl ratios of the freshest waters, while weathering of mafic minerals (e.g., biotite or chlorite) may provide much of the Mg. The weathering reactions described above produce kaolinite, which is common in the Quaternary sediments of the KADA. Molar Na/Cl ratios range from as high as 5.7 in the least saline waters (such as T5) to 0.6–0.7 in the higher salinity waters. Na/Cl molar ratios above 1 likely indicate addition of minor Na by dissolution of albite; these ratios are restricted to fresh ground waters. With increasing salinity, Na/Cl ratios decrease, with most samples having Na/Cl ratios ~1. This could result either due to the increasing dominance of evaporation as the process causing salinization (with Na and Cl concentrations increasing in approximately equal amounts up to seawater-like concentrations and Na/Cl ratios) and/or due to halite dissolution (Herczeg and Edmunds, 2000). However, Cl/Br ratios were measured in samples J2 and S20, and were 440.6 and 304.5, respectively. Halite generally has Cl/Br ratios of $\sim 10^4$ (McCaffrey et al., 1987; Kloppmann et al., 2001; Cartwright et al., 2004), hence, the amount of halite dissolution must be minor. Na/Cl ratios below ~1 that occur in the most saline groundwater probably result from cation exchange of Na for Ca, Mg or Na, as is common in high salinity groundwater where aquifers have high clay contents.

5.4.3. Stable isotopic composition of groundwater

The isotopes of oxygen $\delta^{18}O$ and hydrogen δ^2H in the water molecule are commonly employed as tracers for determining the origin of groundwater and are widely used in studying water circulation and groundwater movement (Ali, 2004) and sources of groundwater salinity (Clark and Fritz, 1997). The oxygen and hydrogen isotopic compositions of KADA shallow groundwater range from −13.3‰ to −4.2‰ and −95‰ to −46‰, respectively (Table 1). A plot of δ^2H and $\delta^{18}O$ in groundwater from the KADA is given in Fig. 15. The δ^2H and $\delta^{18}O$ values generally increase with increasing salinity. The local meteoric water line (LMWL, $\delta^2H = 7.2 \times \delta 18O + 4.3$), which is similar to the global meteoric water line (GMWL; Craig, 1961), is composed of weighted mean $\delta^{18}O$ and δ^2H values of modern rainfall, monitored over 10 years at Urumqi station (43.75°N and 87.60°E), located 280 km southeast of Karamay, as part of the Global Network for Isotopes in Precipitation (http://isohis.iaea.org). The mean values of $\delta^{18}O$ and δ^2H in precipitation are −10.7‰ and −74.1‰, respectively; in groundwater from 10 to 15 m depth, the mean values are −9.7‰ and −77‰, respectively; while in groundwater from 30 to 60 m depth the means are −8.3‰ and −68‰, respectively.

Some groundwater samples, and the irrigation water (I_2) from the IrtySh River plot close to the LMWL, indicating a local meteoric water origin (Fig. 15). In this study area, lateral groundwater re-

Table 4
Parameters used to estimate lateral groundwater recharge in the KADA and resulting estimations.

Section No.	Boundary feature	B (km)	I	H(m)	*k* (m/d)	α (°)	Q (m^3/d)	Q (m^3/a)
1	In-flow	4.67	0.0022	9.3	6.61	90	635.2	231855.3
2	In-flow	4.37	0.0013	5	0.91	90	26.4	9632.4
3	In-flow	4.07	0.0028	6.5	0.016	90	1.2	439.3
4	In-flow	3.01	0.0029	10.6	4.31	90	406.1	148225.6
5	In-flow	3.92	0.0009	10.6	0.35	30	6.9	2514.8
6	In-flow	4.97	0.0019	11	3.06	90	317.4	115838.5
7	In-flow	2.86	0.0007	15	0.41	45	9.2	3350.9
8	In-flow	3.77	0.0008	13.6	16.3	60	599.9	218977.8
9	Out-flow	5.27	0.0012	12.5	3.86	90	307.0	112071.6
10	Out-flow	1.66	0.0025	11	0.29	90	13.0	4743.6
11	Out-flow	3.32	0.0009	16.4	0.02	90	1.0	376.3
12	Out-flow	2.56	0.0072	8.5	1.16	90	182.2	66501.4
13	Out-flow	3.47	0.0046	9.6	0.26	90	39.9	14576.6

Please cite this article in press as: Han, D., et al. A survey of groundwater levels and hydrogeochemistry in irrigated fields in the Karamay Agricultural Development Area, northwest China: Implications for soil and groundwater salinity resulting from surface water transfer for irrigation. J. Hydrol. (2011), doi:10.1016/j.jhydrol.2011.03.052

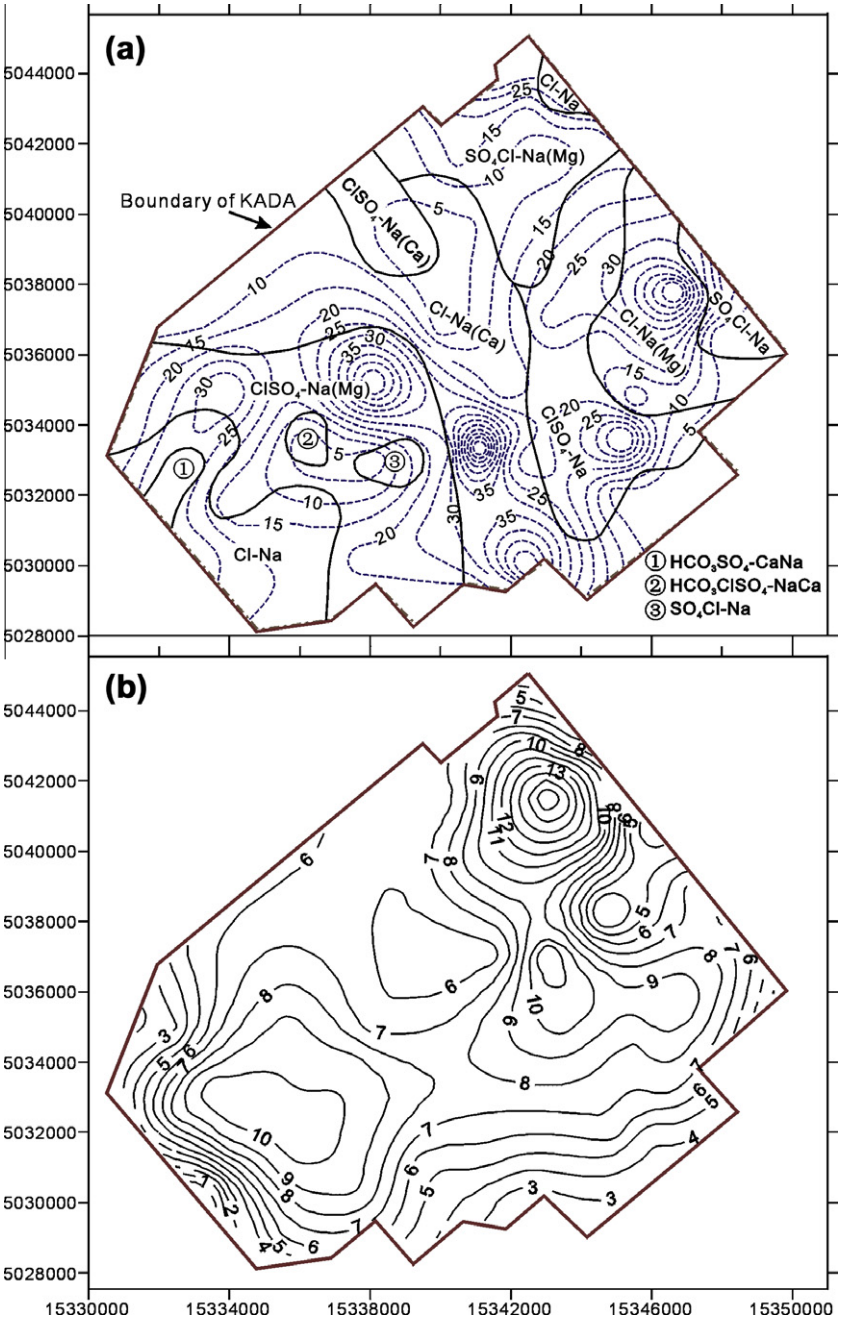

Fig. 10. (a) Hydrochemical zones and TDS contours (in g/L) of shallow groundwater in KADA, Oct.2009; (b) contours of amplitude of shallow groundwater table change (m) from September 1997 to September 2009. In (a), solid black lines are the hydrochemical zone limits and dashed lines are TDS contours.

charge (e.g. from the regional flow system, including mountainous recharge areas) and the water from the IrtySh River tend to carry water into the KADA that is derived from precipitation at much higher altitudes, and is therefore depleted in heavy isotopes (Fig. 15). However, most groundwater samples, including the majority of groundwater from the shallow alluvial aquifer in the irrigation areas, are enriched in $\delta^{18}O$ compared to rain water and the river water, and deviate to the right of the LMWL indicating modification due to evaporation. Generally, the samples that have the highest $\delta^{18}O$ values are highly saline, confirming that evaporation plays important role in the salt accumulation in shallow groundwater. Dilution of shallow groundwater with irrigation water (river water) that has relatively low $\delta^{18}O$ and $\delta^{2}H$ values is probably responsible for the relatively low $\delta^{18}O$ and $\delta^{2}H$ values at 10–15 m depth, while the higher $\delta^{18}O$ and $\delta^{2}H$ values between 30 and 60 m depth could be a result of evaporation during downward infiltration of recharge prior to the irrigation transfer period. This recharge may have been local meteoric water or surface water with higher original $\delta^{18}O$ and $\delta^{2}H$ values than the present-day transferred irrigation water.

An evaporation trend line or lines can be drawn from the intersection of the surface water sample I_2 and the majority of the shallow groundwater samples, plotting above and to the right of this sample. This indicates that groundwater likely contains a significant component of irrigation water that has undergone evaporation before infiltration. Direct evaporation from shallow water tables is also expected to have occurred where the water table has reached 4 m of the ground surface. Partial evaporation of

Please cite this article in press as: Han, D., et al. A survey of groundwater levels and hydrogeochemistry in irrigated fields in the Karamay Agricultural Development Area, northwest China: Implications for soil and groundwater salinity resulting from surface water transfer for irrigation. J. Hydrol. (2011), doi:10.1016/j.jhydrol.2011.03.052

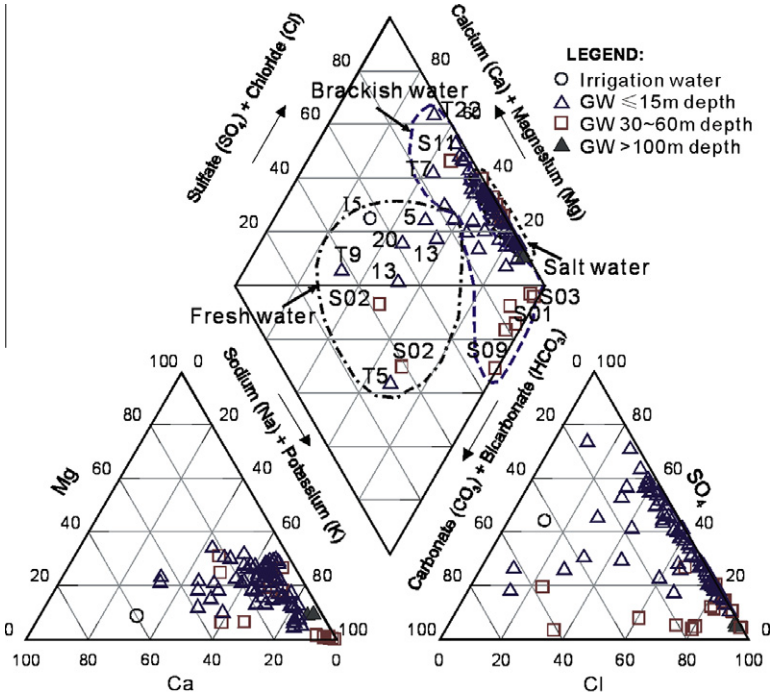

Fig. 11. Piper plot for waters sampled in October 2009 in the KADA.

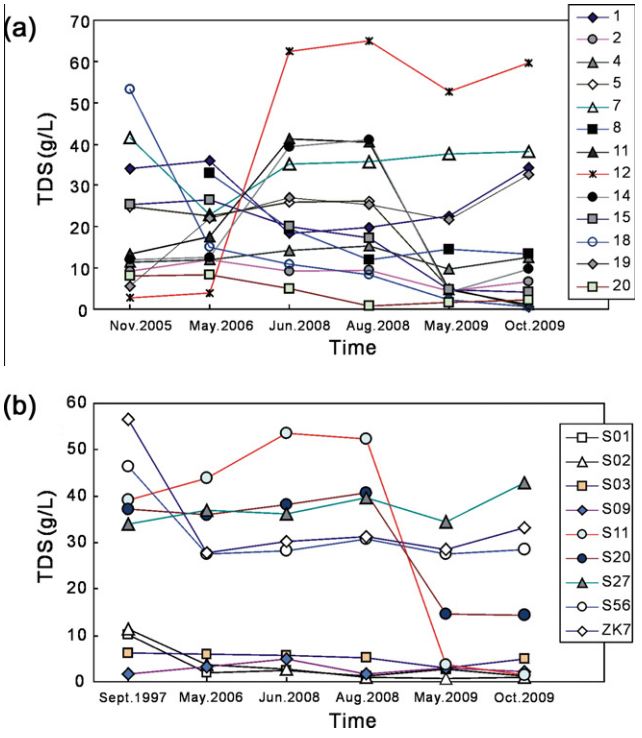

Fig. 12. Variation of groundwater TDS concentrations in the wells of 15 m depth (a) and 30–50 m (S-), 100.5 m (ZK7) depth (b).

infiltrating water in the unsaturated zone and subsequent downward flow and mixing would cause enrichment in groundwater $\delta^{18}O$ values, while complete evaporation of the infiltrating water would result in no net change in the $\delta^{18}O$ values, as the O in water molecules would be lost. The groundwater data show a moderate degree of scatter and a wide range of enrichment (to the right the meteoric water line) that cannot always be traced back to the LMWL along an evaporation trend line to the irrigation water composition. Shallow groundwater thus probably reflects evaporation of water from a variety of recharge sources, including the river water, as well as local precipitation events with a range of different stable isotope compositions along the LMWL, and possibly also some lateral in-flow of groundwater. The scatter in the $\delta^{18}O$ and $\delta^{2}H$ values is greatest in the shallow wells (<15 m) indicating that these waters have not mixed sufficiently to homogenize variations in isotopic composition of various recharge waters.

A local evaporation line was fitted for Aug. 2008 and Oct. 2009, using the following least squares fit linear regression equations: $\delta^{2}H = 5.72 \times \delta 18O - 24.2$ ($n = 48$, $r^2 = 0.91$) in August 2008 and $\delta^{2}H = 5.76 \times \delta 18O - 17.5$ ($n = 49$, $r^2 = 0.88$) in October 2009 (Fig. 15). The two evaporation lines have a very similar *slope*, but the *intercept* is lower on the 2008 line. This suggests that the degree of evaporation, and the humidity at which it occurred was broadly similar in the two periods, but that the starting composition prior to evaporation was different (e.g. due to differences in irrigation water composition). The slightly lesser degree of evaporation in the 2009 samples may also have resulted from the slightly lower groundwater table in October 2009 compared to August 2008.

The deuterium excess ("*d*-excess"), defined by Dansgaard (1964) as $d = \delta 2H - 8\,\delta^{18}O$, allows further insight into the evolution of groundwater salinity to be gained. For the GMWL of Craig (1961), the *d*-excess is 10. Fig. 13 also shows the relationship between $\delta^{18}O$ and the *d*-excess (generally changing between +10‰ and −20‰) in the groundwater. In general $\delta^{18}O$ was negatively correlated with the *d*-excess (Fig. 16). The *d*-excess value is another index of the evaporation effect on the physicochemical characteristics of water: that is, if the water evaporates, the *d*-excess generally decreases. It is probable that only large rainfall events with lower stable isotope compositions are able to recharge groundwater in very dry regions (Tsujimura et al., 2007), such as the KADA. Accordingly, some groundwater in KADA has relatively low $\delta^{18}O$ values (e.g. due to being derived from recharge of precipitation with low $\delta^{18}O$ values) and higher *d*-excess values – which indicate

Please cite this article in press as: Han, D., et al. A survey of groundwater levels and hydrogeochemistry in irrigated fields in the Karamay Agricultural Development Area, northwest China: Implications for soil and groundwater salinity resulting from surface water transfer for irrigation. J. Hydrol. (2011), doi:10.1016/j.jhydrol.2011.03.052

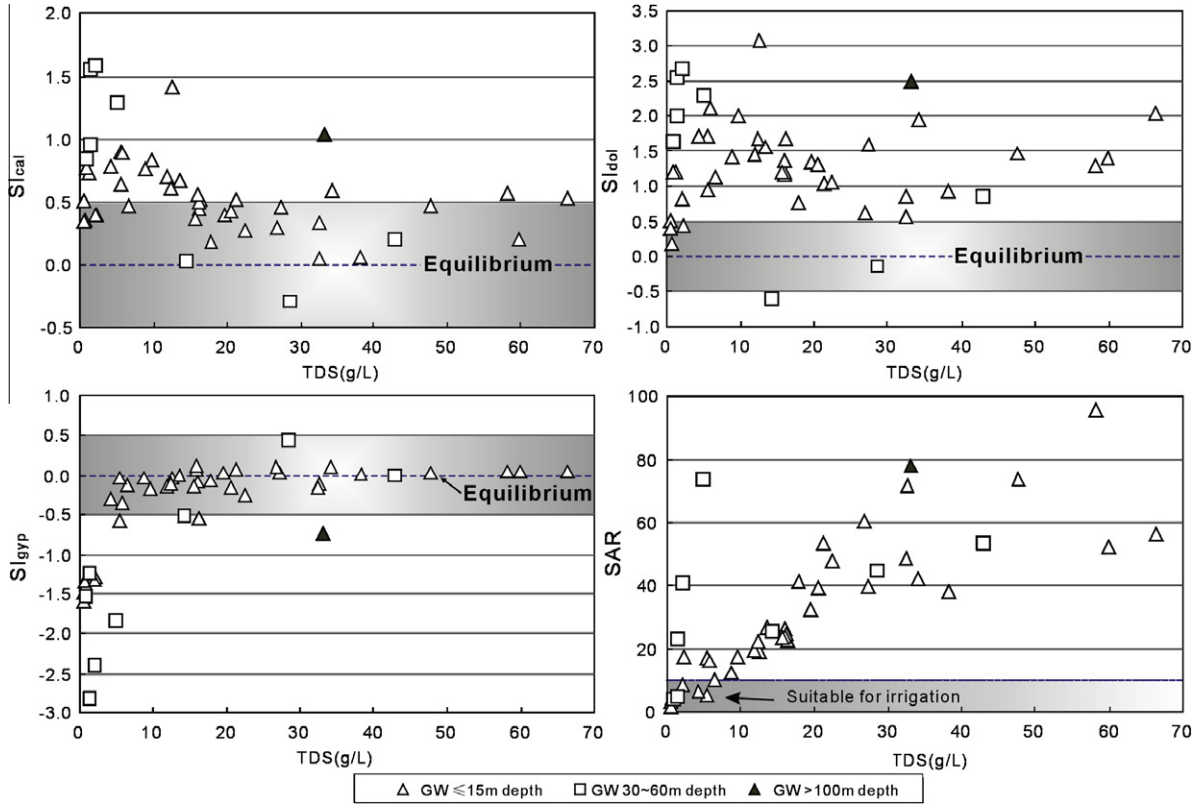

Fig. 13. Variations of calcite- dolomite- and gypsum saturation indices, and sodium adsorption rate (SAR) of analysed groundwater samples in different depth. The saturation indices for calcite (SI_{cal}), dolomite (SI_{dol}) and gypsum (SI_{gyp}) were calculated by the PHREEQCI software (version 2.13.2) (Parkhurst and Appelo, 1999).

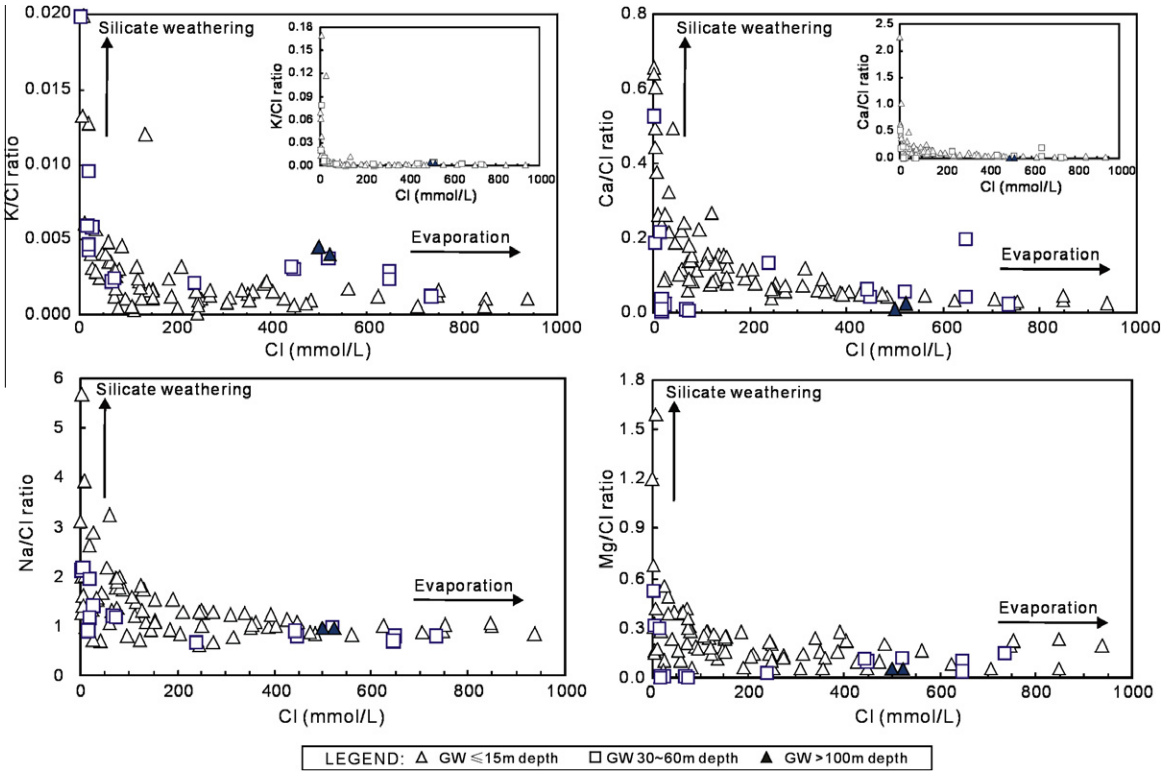

Fig. 14. Variations of major ion/ chloride ratios (K/Cl, Ca/Cl, Na/Cl, and Mg/Cl) with increasing salinity (expressed as Cl concentration).

Please cite this article in press as: Han, D., et al. A survey of groundwater levels and hydrogeochemistry in irrigated fields in the Karamay Agricultural Development Area, northwest China: Implications for soil and groundwater salinity resulting from surface water transfer for irrigation. J. Hydrol. (2011), doi:10.1016/j.jhydrol.2011.03.052

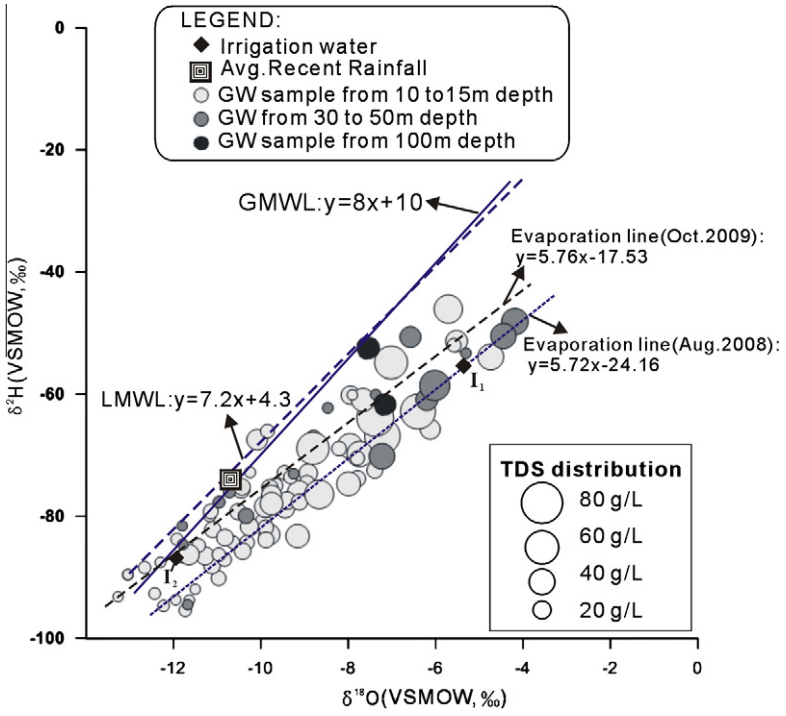

Fig. 15. Plot of stable isotopes from rainfall, irrigation water and groundwater from the KADA. "Avg. Recent Rainfall" refers to the weighted average isotopic composition of rainfall in Urumuqi station of IAEA networks since 1986–2003. The total dissolved solids (TDS) content of each sample is also indicated by the size of the point.

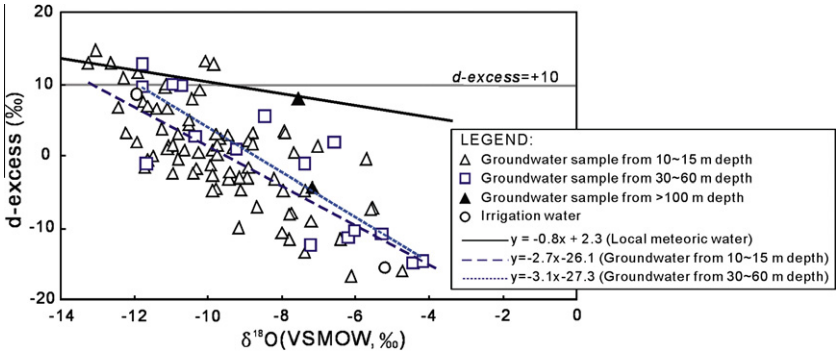

Fig. 16. Plot of *d-excess* vs. $\delta^{18}O$ for various water samples.

that evaporation has still been extensive, in spite of the waters still having relatively low $\delta^{18}O$ values.

Another complicating factor which may apply due to the extreme aridity of the area is that in the event of very intensive evaporation removing all of the water in the soil, the isotopic evaporation signals do not remain in the soil water or groundwater because $\delta^{18}O$ and $\delta^{2}H$ constitute the water molecules themselves. Thus, under highly dry conditions, the stable isotopes in the groundwater can be biased towards more depleted compositions (Tsujimura and Tanaka, 1998). Consequently, because only relatively large rainfall/irrigation events can recharge the groundwater and the effect of the large amount of evaporation does not remain in the subsurface water, the groundwater can have relatively low $\delta^{18}O$ and $\delta^{2}H$ compositions but high d-excess values, which still indicate that evaporation has occurred.

5.5. Management of shallow groundwater and soil salinity

Although the salinity of shallow groundwater in the KADA temporarily decreases when surface water is transferred to the area, the groundwater table rise has exacerbated the development of saline soil, and the overall salt load is increasing, and moving closer to the soil zone. Water management in arid regions is inseparably coupled to salt management. According to the results of water budget analysis in the area, irrigation infiltration occupied over 90% of the total recharge of the shallow aquifers in KADA. Reduction of the irrigated area or change to alternative crops could reduce the extent of the water table rise and salt accumulation. Development of groundwater-pumping and disposal of the water into evaporation basins (on land that is not used or earmarked for agriculture, industry or residential development) may be effective in lowering the water tables in the region and limiting the extent of soil salinity. This option provides a way of exporting salts from the region, which could potentially be harvested as a new local industry. However, the effectiveness of pumping in reducing the shallow groundwater table will depend upon hydraulic properties of the aquifer – e.g. pumping at depth will be most effective where there is no clay barrier between shallow and deeper units, such as in the palaeochannel areas.

Please cite this article in press as: Han, D., et al. A survey of groundwater levels and hydrogeochemistry in irrigated fields in the Karamay Agricultural Development Area, northwest China: Implications for soil and groundwater salinity resulting from surface water transfer for irrigation. J. Hydrol. (2011), doi:10.1016/j.jhydrol.2011.03.052

Using advanced irrigation equipment for water-saving could also result in limiting the rise in water tables, however, unless water brought in to the area by transfer of river water is reduced or balanced by removal of water (e.g. via pumping and disposal), the overall salt load in the area is still likely to increase and move towards the surface. Subsurface drainage systems, such as digging drainage ditches treated by anti-seepage, could also be designed to prevent residual soil water from recharge into shallow aquifer and maintain a lower water table, thereby avoiding concentration of salts in the root zone. Additionally, planting trees, such as poplar and desert date, can be regarded as "biological drainage" playing an important role in water table control (although the salt tolerance of the plants is limited, and the plants cannot remove salts, only water). Careful consideration and adoption of appropriate water management practices may yet be able to avoid irreversible and quasi-irreversible damage to the productivity and health of the local agricultural and ecological environment.

In addition to counter-measures for managing shallow groundwater and controlling soil salinity, further specific research could be performed, such as building models for drivers of shallow water table, and water-salt balance models.

6. Conclusions

The KADA presents a case study of arid-region groundwater salinization under the influence of agricultural irrigation from transferred surface water. In this research, physical data (e.g. water level changes, geologic data) were used to characterize the water budget in the region, and the various factors that are important in controlling water levels. Over irrigation in KADA has led to substantial groundwater level rise in the shallow aquifer. The mean rise of groundwater table was 6.9 m from September 1997 to September 2009. The accumulated total net storage change is close to 150 million cubic meters from September 1997 to September 2009. Irrigation was found to constitute >90% of recharge, while evapotranspiration is the primary discharge mechanism.

Chemical analysis of groundwater samples collected from the KADA was also carried out in order to investigate the hydrochemistry of the Quaternary shallow aquifer and better characterize the quality impacts of irrigation on the groundwater. In most of the shallow groundwater the TDS and Cl concentrations are high (mean values of 20 and 8.3 g/L, respectively); ~65% of sampled waters are classed as salt water (>10 g/L) and are Cl(SO_4)–Na type. Solutes in groundwater in the KADA are derived by evapotranspiration of shallow groundwater with minor rock weathering, halite dissolution, and possibly ion exchange. Gypsum and calcite precipitation are likely responsible for the trend towards Na–Cl dominated major ion chemistry with increasing salinity. The calculated SAR results for shallow groundwater indicate that most water is not suitable for irrigation. That saline groundwater dominantly occurs in regions of low hydraulic conductivity between palaeochannels, suggests that the variation in salinity may be due to the rate at which groundwater recharges.

Stable isotope data show that much of the shallow groundwater in KADA is enriched in $\delta^{18}O$, deviating from the LMWL, indicating infiltration of irrigation water that had undergone evaporation. Some groundwater has relatively low $\delta^{18}O$ values and higher *d*-excess, suggesting the waters that recharged the aquifer (e.g. from very heavy rain events or transferred surface water) had lower initial $\delta^{18}O$ values, but were still subject to evaporation. The data in this paper can provide an important basis for the further study of the groundwater environment in the KADA, and other analogous regions. Further characterization of the water and salt balance in the area could be achieved using additional geochemical and geophysical information, and there is potential for modeling as the density of monitoring data increases over subsequent years.

Acknowledgements

This work was supported by the West Planning Action Program (No.KZCX2-XB2-13) of the Chinese Academy of Sciences, entitled "Water Saving Irrigation for water-salt adjustment and control in the saline land of North China" and was financially supported by the National Natural Science Foundation of China (No. 40801018). The authors would like to thank Mr.Meng, Director of the office of Karamay Agricultural Development for providing important information on the groundwater in KADA. Thanks are also to Mr.Chang Fuhai for support in the field survey.

References

Ali, M. Subyani, 2004. Use of chloride-mass balance and environmental isotopes for evaluation of groundwater recharge in the alluvial aquifer, Wadi Tharad, west Saudi Arabia. Environmental Geology 46, 741–749.

Allison, G.B., Cook, P.G., Barnett, S.R., Walker, G.R., Jolly, I.D., Hughes, M.W., 1990. Land clearance and river salinisation in the Murray Basin, Australia. Journal of Hydrology 119, 1–20.

Arad, A., Evans, R., 1987. The hydrogeology, hydrochemistry and environmental isotopes of the Campaspe River aquifer system, north-central Victoria, Australia. Journal of Hydrology 95, 63–86.

Cartwright, I., Weaver, T.R., Fulton, S., Nichol, C., Reid, M., Cheng, X., 2004. Hydrogeochemical and isotopic constraints on the origins of dryland salinity, Murray Basin, Victoria, Australia. Applied Geochemistry 19, 1233–1254.

Cartwright, I., Weaver, T.R., Stone, D., Reid, M., 2007. Constraining modern and historical recharge from bore hydrographs, ^{3}H, ^{14}C and chloride concentrations: applications to dual-porosity aquifers in dryland salinity areas, Murray Basin, Australia. Journal of Hydrology 332, 69–92.

Chappell, N.A., Ternan, J.L., Bidin, K., 1999. Correlation of physicochemical properties and sub-erosional landforms with aggregate stability variations in a tropical Ultisol disturbed by forestry operations. Soil & Tillage Research 50, 55–71.

Clark, I.D., Fritz, P., 1997. Environmental Isotopes in Hydrogeology. Lewis Publishers, Boca Raton, pp. 144–207.

Craig, H., 1961. Standard for reporting concentration of deuterium and oxygen-18 in natural water. Science 133, 1833–1834.

Cui, D., Liu, Z.Y., Luo, Z.H., Wen, J., 1997. Hydrogeological survey report of ecological agricultural are in Karamay arid region 9–11.

Dansgaard, W., 1964. Stable isotopes in precipitation. Tellus 16, 436–438.

De Vries, J.J., Simmers, I., 2002. Groundwater recharge: an overview of processes and challenges. Hydrogeology Journal 10, 5–17.

Edmunds, W.M., Ma, J., Aeschbach-Hertig, W., Kipfer, R., Darbyshire, D.P.F., 2006. Groundwater recharge history and hydrogeochemical evolution in the Minqin Basin, North West China. Applied Geochemistry 21 (12), 2148–2170.

Fetter, C.W., 1994. Applied hydrogeology. Prentice Hall, Englewood Cliffs.

Froehlich, K., Yurtsever, Y., 1995. Isotope techniques for water resources in arid and semiarid regions. In: Adar, E.M., Leibundgut, C. (Eds.), Application of Tracers in Arid Zone Hydrology (Proceedings of the Vienna Symposium. IAHS Publ.no.232:3–12, August 1994.

Gates, J.B., Bohlke, J.K., Edmunds, W.M., 2008. Ecohydrological factors affecting nitrate concentrations in a phreatic desert aquifer in northwestern China. Environmental Science and Technology 42, 3531–3537.

Healy, R.W., Cook, P.G., 2002. Using groundwater levels to estimate recharge. Hydrogeology Journal 10, 91–109.

Herczeg, A.L., Edmunds, W.M., 2000. Inorganic ions as tracers. In: Cook, P., Herczeg, A. (Eds.), Environmental Tracers in Subsurface Hydrology. Kluwer Academic Publishers, Boston, pp. 31–77.

Kloppmann, W., Négrel, Ph., Casanova, J., Klinge, H., Schelkes, K., Guerrot, C., 2001. Halite dissolution derived brines in the vicinity of a Permian salt dome (N German Basin). Evidence from boron, strontium, oxygen, and hydrogen isotopes. Geochimica et Cosmochimica Acta 65, 4087–4101.

Mao, J.M., Tian, C.Y., Wen, Q.K., Wu, H.Q., Wang, X.Y., Zhang, S.Y., 2007. Study on soil qualitative characteristics of different land utilization way in agricultural development zones of Karamay. Journal of Xinjiang Agricultural University 30 (2), 41–44 (in Chinese).

McCaffrey, M.A., Lazar, B., Holland, H.D., 1987. The evaporation path of seawater and the coprecipitation of Br^{-} and K^{+} with halite. Journal of Sedimentary Petrology 57, 928–937.

Nonner, J.C., 2006. Introduction to Hydrogeology. Taylor & Francis Group plc, London, UK, p186.

Parkhurst, D.L., Appelo, C.A.J., 1999. User's guide to PHREEQC-a computer program for speciation, reaction-path, 1D-transport, and inverse geochemical calculation: US Geological Survey. Water-Resour Investig Rep 99-4259, 312.

Simpson, H.J., Herczeg, A.L., 1991. Salinity and evaporation in the River Murray Basin, Australia. Journal of Hydrology 124, 1–27.

Stadler, S., Osenbrück, K., Suckow, A.O., Himmelsbach, T., Hötzl, H., 2010. Groundwater flow regime, recharge and regional-scale solute transport in the

Please cite this article in press as: Han, D., et al. A survey of groundwater levels and hydrogeochemistry in irrigated fields in the Karamay Agricultural Development Area, northwest China: Implications for soil and groundwater salinity resulting from surface water transfer for irrigation. J. Hydrol. (2011), doi:10.1016/j.jhydrol.2011.03.052

semi-arid Kalahari of Botswana derived from isotope hydrology and hydrochemistry. Journal of Hydrology 388, 291–303.

Tsujimura, M., Tanaka, T., 1998. Evaluation of evaporation rate from forested soil surface using stable isotopic composition of soil water in a headwater basin. Hydrological Processes 12, 2093–2103.

Tsujimura, M., Abe, Y., Tanaka, T., Shimada, J., Higuchi, S., Yamanaka, T., Davva, G., Oyunbaatar, D., 2007. Stable isotopic and geochemical characteristics of groundwater in Kherlen River basin, a semi-arid region in eastern Mongolia. Journal of Hydrology 333, 47–57.

Wang, X.Y., Tian, C.Y., Wen, Q.K., Wu, H.Q., Mao, J.M., 2007. Influence of land utilization way on soil salt in Karamay agricultural development zones. Journal of Xinjiang Agricultural University 30 (2), 38–40, in Chinese.

World Health Organisation, 1984. Guidelines for Drinking Water Quality, vol. 1. World Health Org., Geneva.

Yao, X.R., Pan, C.D., Zhang, H.H., Li, D.M., Chang, F.H., 2008. Study on the water-soil environmental characteristics in Karamay agricultural development region after land exploitation. Journal of Xinjiang Agricultural University 31 (1), 1–6 (in Chinese).

Please cite this article in press as: Han, D., et al. A survey of groundwater levels and hydrogeochemistry in irrigated fields in the Karamay Agricultural Development Area, northwest China: Implications for soil and groundwater salinity resulting from surface water transfer for irrigation. J. Hydrol. (2011), doi:10.1016/j.jhydrol.2011.03.052